Projected Stein variational methods for high-dimensional Bayesian inversion

Peng Chen

Oden Institute for Computational Engineering and Sciences
The University of Texas at Austin

May 2, 2020

Example I: inversion in Antarctica ice sheet flow

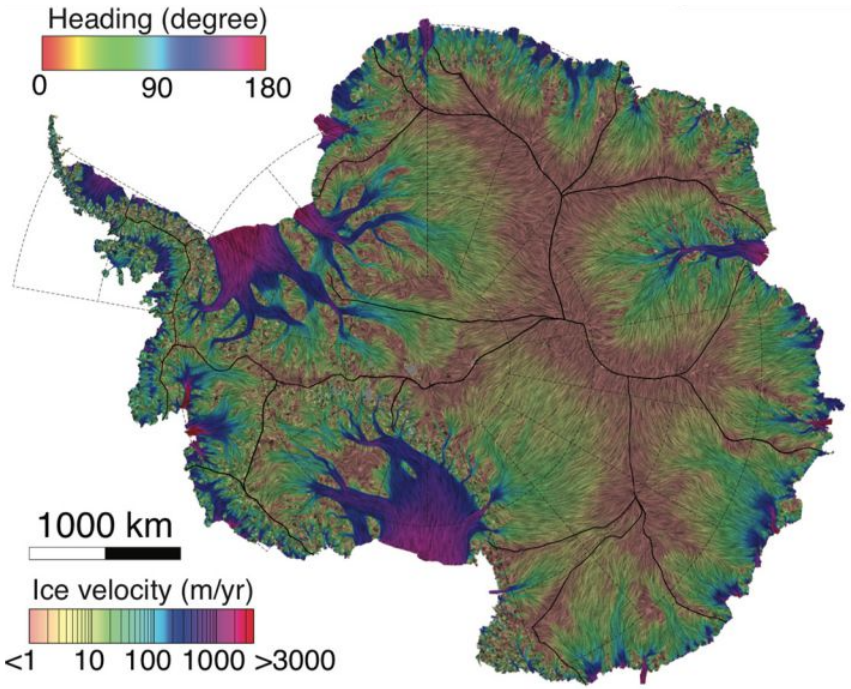

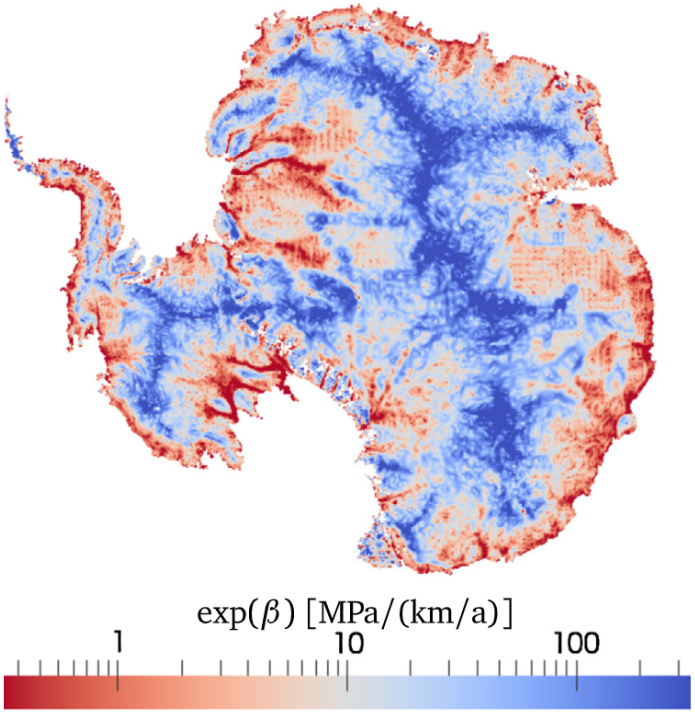

- Model: nonlinear viscous, incompressible fluid flow.
- Parameter: basal sliding field in boundary condition.
- Data: (InSAR) satellite observation of surface ice flow velocity.

T. Isaac, N. Petra, G. Stadler, O. Ghattas, JCP, 2015

Ongoing with: T. O'Leary-Roseberry, U. Villa, O. Ghattas

Example II: inversion in gravitational wave propogation

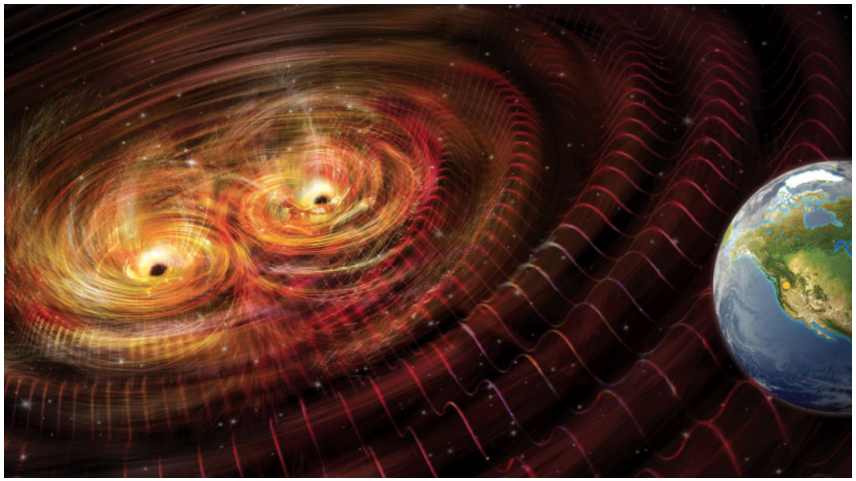

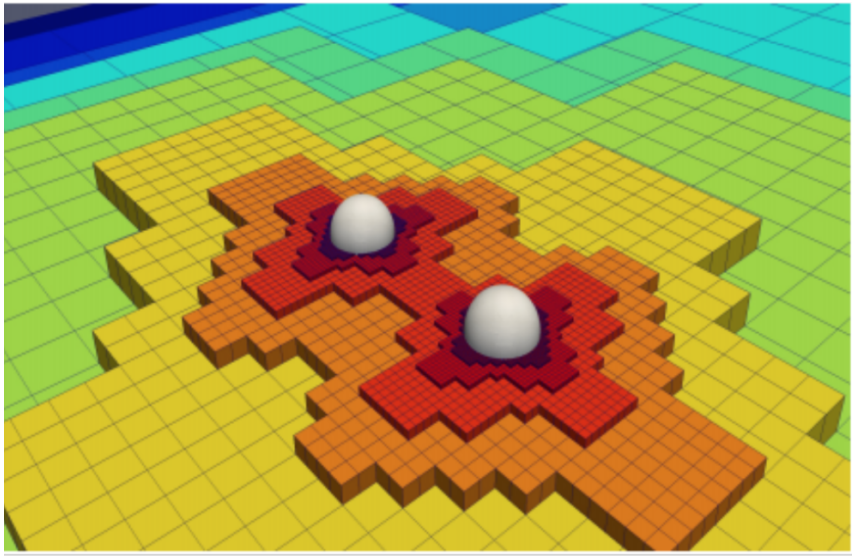

- Model: Eienstein field equations, approximate models.
- Parameter: mass ratio, location of black holes, etc.
- Data: LIGO/Virgo observation of the gravitational waves on earth.

M. Fernando, D. Neilsen, H. Lim, E. Hirschmann, H. Sundar, SISC, 2019.

Ongoing with: B. Saleh, A. Leviyev, J. Chen, A. Zimmerman, O. Ghattas

Example III: inversion in COVID-19 pandemic

Country, Other	Total Cases	New Cases	Total Deaths	New Deaths
World	2,467,519	+60,944	169,398	+4,367
USA	784,201	+19,565	41,837	+1,262
Spain	200,210	+1,536	20,852	+399
Italy	181,228	+2,256	24,114	+454
France	155,383	+2,489	20,265	+547
Germany	146,398	+656	4,706	+64
UK	124,743	+4,676	16,509	+449
Turkey	90,980	+4,674	2,140	+123
Iran	83,505	+1,294	5,209	+91
China	82,747	+12	4,632	
Russia	47,121	+4,268	405	+44
Belgium	39,983	+1,487	5,828	+145
Brazil	39,681	+1,027	2,512	+50
Canada	36,670	+1,614	1,680	+93
Netherlands	33,405	+750	3,751	+67
Switzerland	27,944	+204	1,429	+36

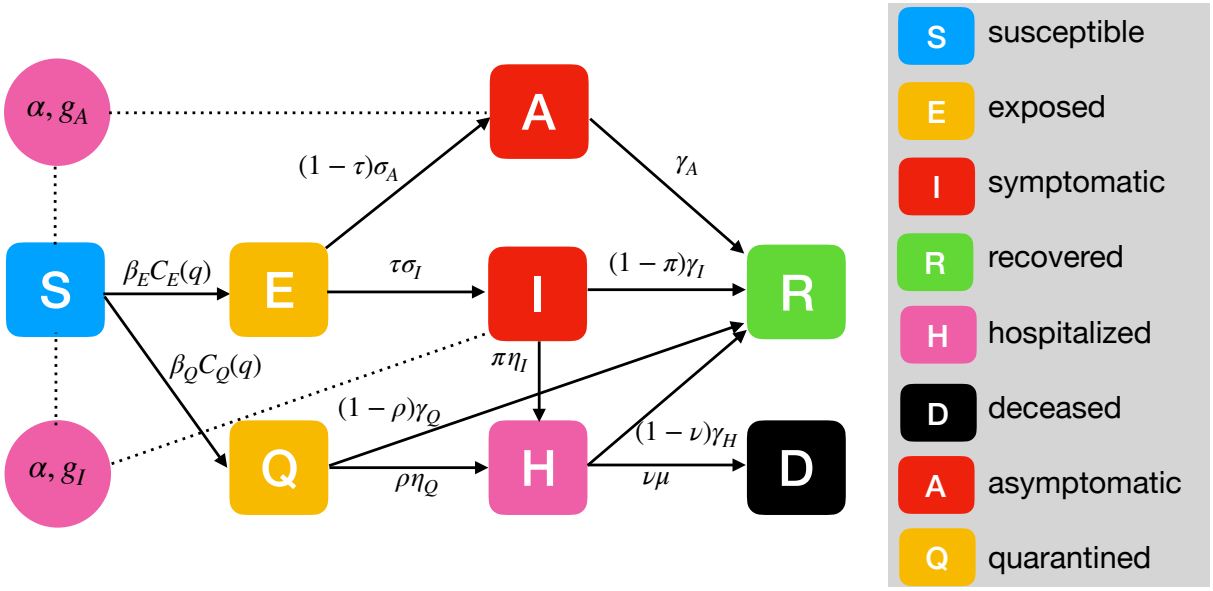

- Model: ODE and network based compartmental models
- Parameter: reproduction number, asymptomatic ratio, transmission/incubation/hospitalization/deceased/recovery rates.
- Data: daily update on confirmed infection, death cases, etc.

Ongoing with: K. Wu, D. Luo, I. Farcas, N. Alger, L. Gao, T. O'Leary-Roseberry, O. Ghattas

Example III: inversion in COVID-19 pandemic

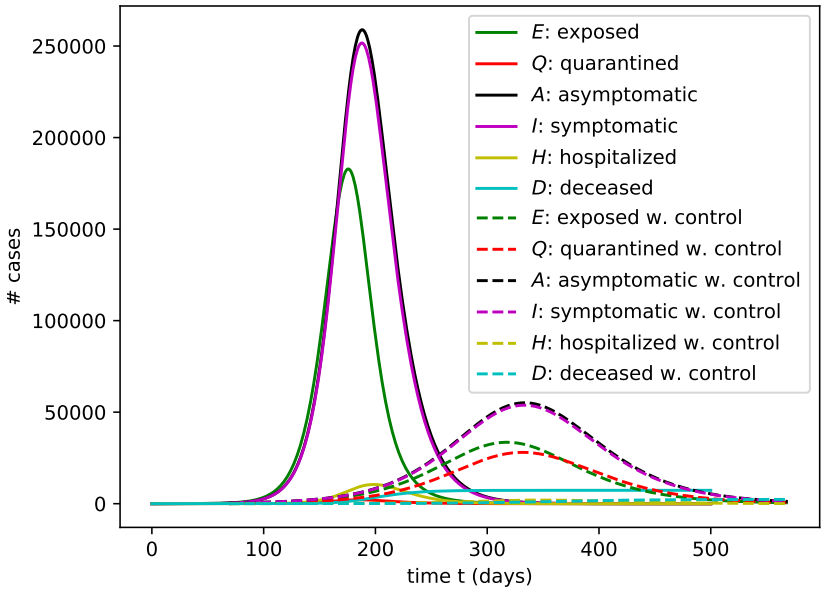

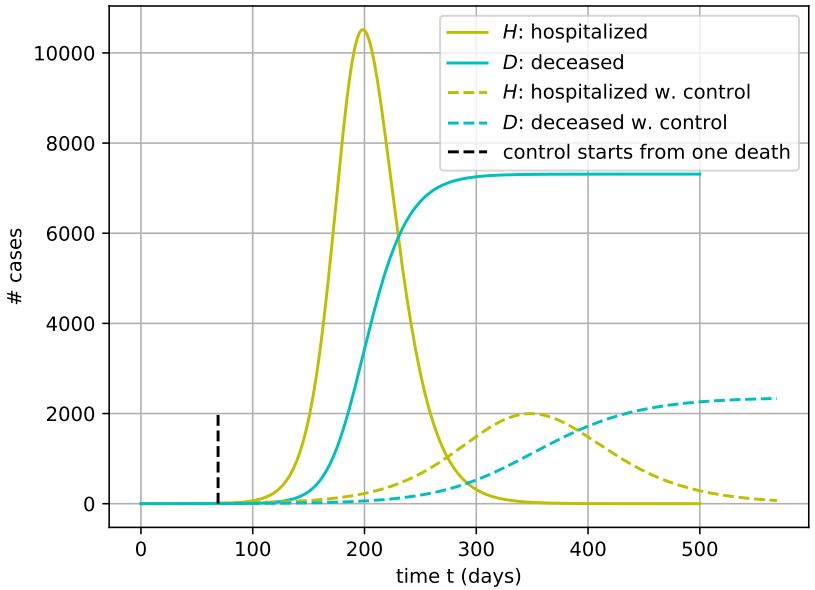

- Model: ODE and network based compartmental models
- Parameter: reproduction number, asymptomatic ratio, transmission/incubation/hospitalization/deceased/recovery rates.
- Data: daily update on confirmed infection, death cases, etc.

Ongoing with: K. Wu, D. Luo, I. Farcas, N. Alger, L. Gao, T. O'Leary-Roseberry, O. Ghattas

Example III: inversion in COVID-19 pandemic

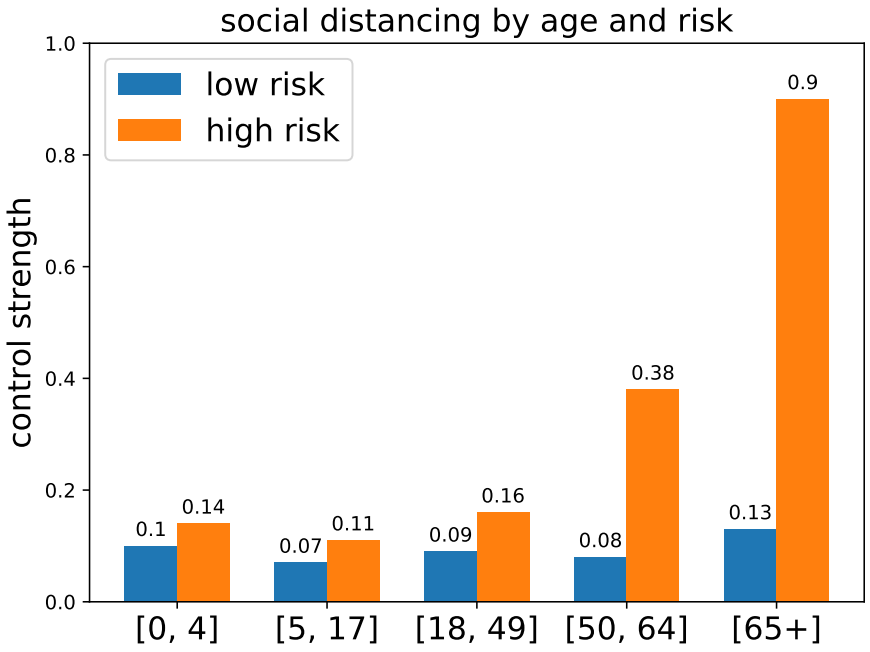

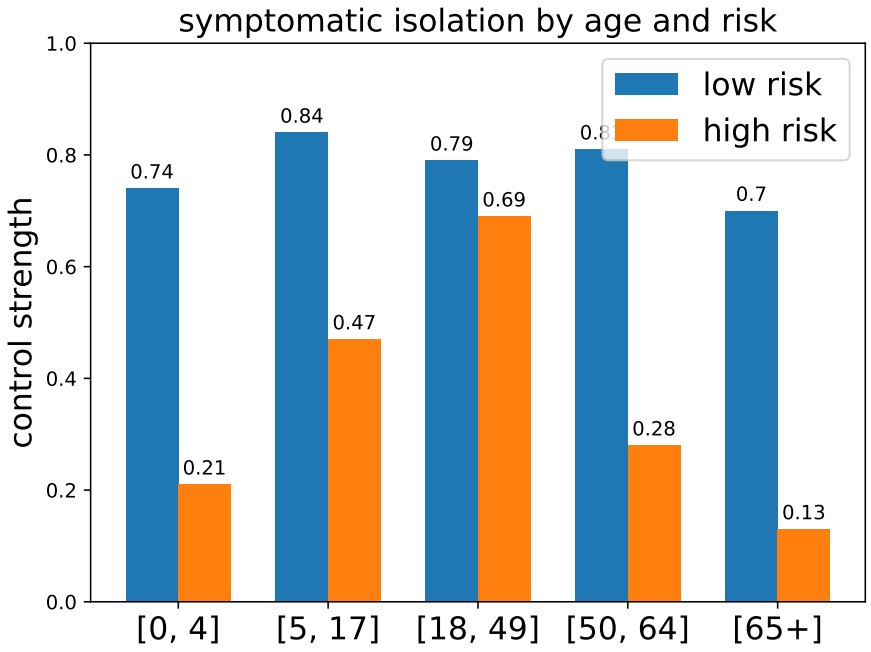

- Model: ODE and network based compartmental models
- Parameter: reproduction number, asymptomatic ratio, transmission/incubation/hospitalization/deceased/recovery rates.
- Data: daily update on confirmed infection, death cases, etc.

Ongoing with: K. Wu, D. Luo, I. Farcas, N. Alger, L. Gao, T. O'Leary-Roseberry, O. Ghattas

Outline

Outline

Bayesian inversion

We consider an abstract form of the parameter to data model

$$y = \mathcal{O}(\theta) + \xi$$

- uncertain parameter: $\theta \in \Theta \subset \mathbb{R}^d$
- parameter-to-observable map $\mathcal{O}$
- observation data: $y \in \mathbb{R}^n$
- noise ξ, e.g., $\xi \sim \mathcal{N}(0, \Gamma)$

Bayes' rule:

$$\underbrace{\pi_y(\theta)}_{\text{posterior}} = \frac{1}{\pi(y)} \underbrace{\pi(y|\theta)}_{\text{likelihood}} \underbrace{\pi_0(\theta)}_{\text{prior}},$$

with the model evidence

$$\pi(y) = \int_\Theta \pi(y|\theta)\pi_0(\theta)d\theta.$$

The central tasks: sample from posterior and compute statistics, e.g.,

$$\mathbb{E}_{\pi_y}[s] = \int_\Theta s(\theta)\pi_y(\theta)d\theta.$$

Computational challenges

Computational challenges for Bayesian inversion:

- the posterior has **complex** geometry:
  non-Gaussian, multimodal, concentrating in a local region
- the parameter lives in **high-dimensional** spaces
  curse of dimensionality – complexity grows exponentially
- the map $\mathcal{O}$ is **expensive** to evaluate:
  involving solve of large-scale partial differential equations

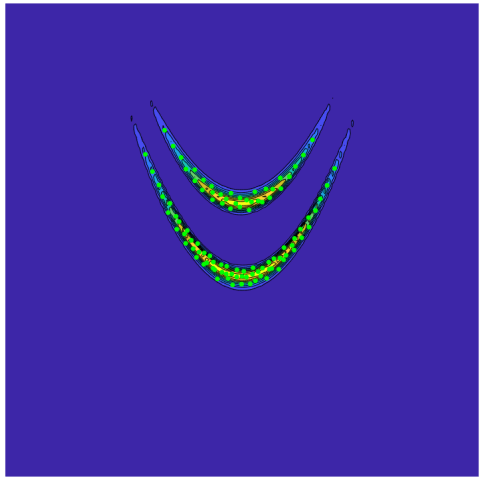

complex geometry

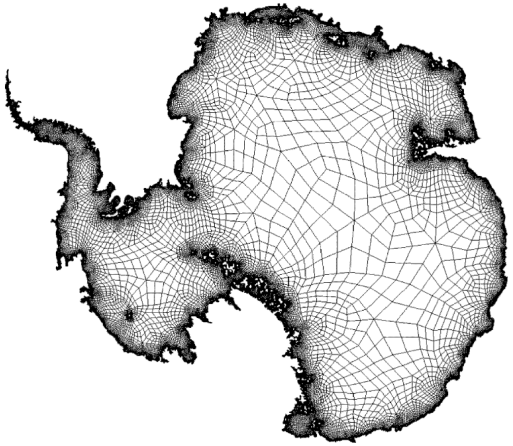

high dimensionality

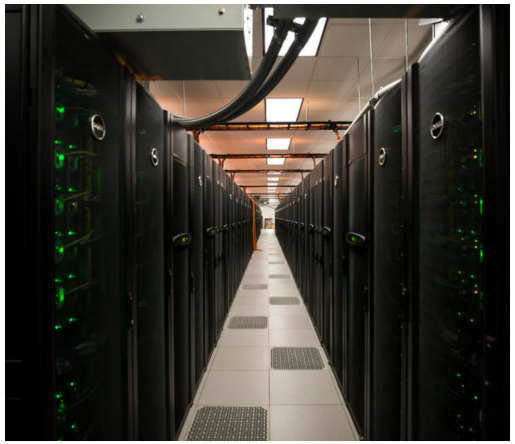

large-scale computation

Computational methods

- **Accelerated MCMC to increase the effective # samples**
  1. Langevin and Hamiltonian MCMC (local geometry using gradient, Hessian, etc.) [Stuart et al., 2004, Girolami and Calderhead, 2011, Martin et al., 2012, Bui-Thanh and Girolami, 2014, Lan et al., 2016, Beskos et al., 2017]...
  2. dimension reduction MCMC (intrinsic low-dimensionality) [Cui et. al., 2014, 2016, Constantine et. al., 2016]...
  3. randomized/optimized MCMC (optimization for sampling) [Oliver, 2017, Wang et al., 2018, Wang et al., 2019]...
- **Direct posterior construction and statistical computation**
  1. Laplace approximation (Gaussian posterior approximation) [Bui-Thanh et al., 2013, Chen et al., 2017, Schillings et al., 2019]...
  2. deterministic quadrature (sparse Smolyak, high-order quasi-MC) [Schillings and Schwab, 2013, Gantner and Schwab, 2016, Chen and Schwab, 2016, Chen et al., 2017]...
  3. transport maps (polynomials, radial basis functions, deep neural networks) [El Moselhy and Marzouk, 2012, Spantini et al., 2018, Rezende and Mohamed, 2015, Liu and Wang, 2016, Detommaso et al., 2018, Chen et al., 2019]...

Computational methods

- **Surrogate models to reduce the large-scale computation**
  1. polynomial approximation (stochastic spectral, stochastic collocation) [Marzouk et al., 2007, Marzouk and Xiu, 2009, Schwab and Stuart, 2012, Chen et al., 2017, Farcas et al., 2019]...
  2. model reduction (POD, greedy reduced basis) [Wang and Zabaras, 2005, Lieberman et al., 2010, Nguyen et al., 2010, Lassila et al., 2013, Cui et al., 2015, Chen and Schwab, 2016, Chen and Ghattas, 2019]...
  3. multilevel/multifidelity (MCMC, stochastic collocation) [Dodwell et. al., 2015, Teckentrup et. al., 2015, Scheichl et. al., 2017, Peherstorfer. et. al., 2018, Farcas et. al., 2019]...

Fast and **scalable** Bayesian inversion in **high** dimensions by exploiting intrinsic low-dimensionality in both parameter and state spaces, using

- projected transport map in parameter space
- reduced basis approximation in state space

Outline

Variational inference by transport

Variational inference: find density $p^* \in \mathcal{P}$ such that

$$p^* = \operatorname*{argmin}_{p \in \mathcal{P}} D(p|\pi_y).$$

by a variational method. Density class by transport $\mathcal{P} = \{T_\sharp \pi_0 : T \in \mathcal{T}\}$.

Find $T : \mathbb{R}^d \to \mathbb{R}^d$, such that $\theta \sim \pi_0 \to T(\theta) \sim \pi_y$.

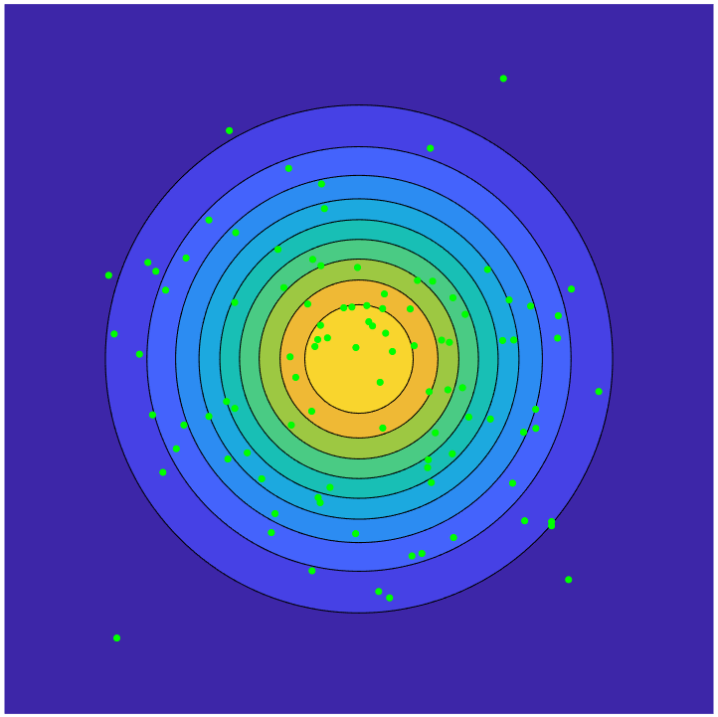

prior

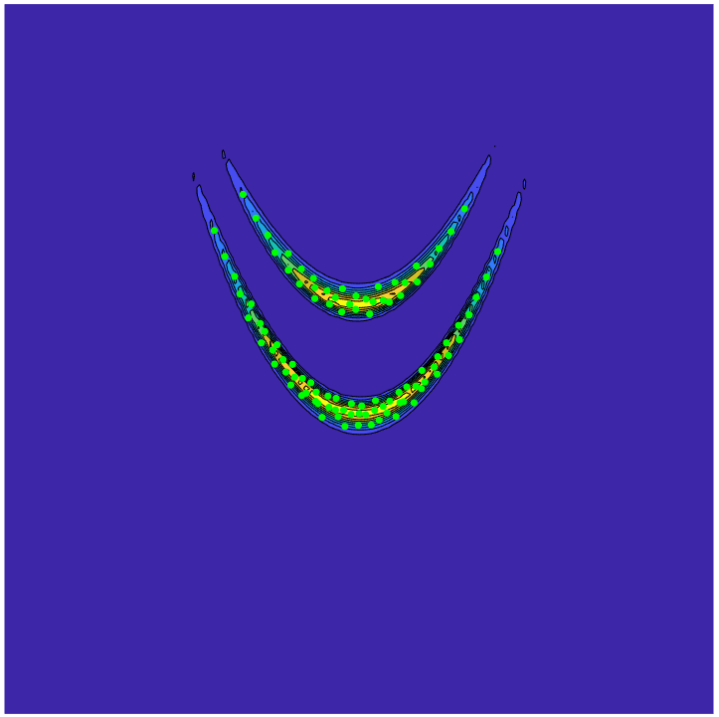

posterior

Optimization for the transport map

- Find a **transport map** $T : \mathbb{R}^d \to \mathbb{R}^d$, such that

$$\theta \sim \pi_0 \to T(\theta) \sim \pi_y,$$

by solving the minimization problem

$$\min_{T \in \mathcal{T}} \mathcal{D}_{\mathsf{KL}}(T_\sharp \pi_0 | \pi_y).$$

- Kullback–Leibler (KL) divergence

$$\mathcal{D}_{\mathsf{KL}}(\pi_1 | \pi_2) = \int_\Theta \pi_1(\theta) \log\left(\frac{\pi_1(\theta)}{\pi_2(\theta)}\right) d\theta.$$

- $T_\sharp$ is a pushforward map such that

$$T_\sharp \pi_0(\theta) = \pi_0(T^{-1}(\theta)) |\mathsf{det} \nabla T^{-1}(\theta)|.$$

- $\mathcal{T}$ is a tensor-product function space $\mathcal{H}^d = \mathcal{H} \otimes \cdots \otimes \mathcal{H}$.

Composition of transport maps

Instead of seeking **one complex (highly nonlinear)** transport map T, we look for **composition of a sequence of simple** transport maps

$$T = T_L \circ T_{L-1} \circ \cdots \circ T_1 \circ T_0, \quad L \in \mathbb{N},$$

- **perturbation of identity**:

$$T_l(\theta) = I(\theta) + Q_l(\theta),$$

- identity map $I(\theta) = \theta$
- perturbation map $Q_l : \mathbb{R}^d \to \mathbb{R}^d$

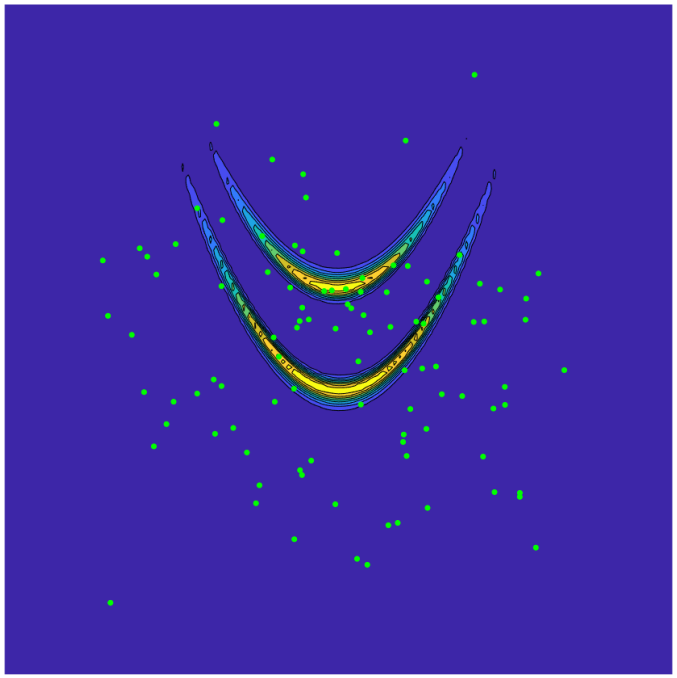

Optimization of each transport map

At each $l = 0, 1, \ldots,$ we define

$$\pi_{l+1} := (T_l \circ \cdots \circ T_0)_\sharp \pi_0 \Longleftrightarrow \pi_{l+1} = (T_l)_\sharp \pi_l$$

We introduce a cost functional

$$\mathcal{J}_l[Q] := \mathcal{D}_{\mathrm{KL}}((I + Q)_\sharp \pi_l | \pi_y). \tag{1}$$

One step optimization of $\mathcal{J}_l(Q)$ w.r.t. Q leads to

$$T_l = I + \alpha_l Q_l,$$

with step size $\alpha_l > 0$ (learning rate, line search).

Optimization methods

- Gradient descent method: steepest descent [Liu and Wang, 2016]

$$Q_l = -D\mathcal{J}_l[\mathbf{0}].$$

- Newton method: solve the linear system [Detommaso et al., 2018]

$$D^2\mathcal{J}_l[\mathbf{0}](V, Q_l) = -D\mathcal{J}_l[\mathbf{0}](V), \quad \forall\, V \in \mathcal{T}.$$

Reproducing Kernel Hilbert Space (RKHS)

Gaussian kernel for RKHS $\mathcal{H}$

$$k(\theta, \theta') = \exp\left(-\frac{1}{2h}(\theta - \theta')^\top \mathbb{M}(\theta - \theta')\right).$$

To account for the geometry of the posterior, [Detommaso et al., 2018]

$$\mathbb{M} = \bar{\mathbb{H}} := \mathbb{E}_{\pi_l}\left[-\nabla_\theta^2 \log(\pi_y(\theta))\right], \; h = d, \quad \text{v.s.} \quad \mathbb{M} = \mathbb{I} \in \mathbb{R}^{d\times d}.$$

Finite dimensional approximation of RKHS:

$$\mathcal{H}_N^l = \text{span}(k_1^l(\theta), \ldots, k_N^l(\theta)) \subset \mathcal{H},$$

where the basis functions are taken as

$$k_n^l(\theta) = k(\theta, \theta_n^l), \quad n = 1, \ldots, N,$$

where $\theta_n^l \sim \pi_l$ are particles transported from $\theta_n^0 \sim \pi_0$ by

$$\theta_n^l = (T_l \circ \cdots \circ T_0)(\theta_n^0), \quad n = 1, \ldots, N.$$

Stein variational gradient descent (SVGD)

[Liu and Wang, 2016]

- For $D\mathcal{J}_l[\mathbf{0}](V) = \langle D\mathcal{J}_l[\mathbf{0}], V\rangle_{\mathcal{H}^d}$, by the reproducing property

$$\langle D\mathcal{J}_l[\mathbf{0}], V\rangle_{\mathcal{H}^d} = -\langle \mathbb{E}_{\pi_l}[\nabla_\theta \log(\pi_y(\theta))k(\theta,\theta') + \nabla_\theta k(\theta,\theta')], V(\theta')\rangle.$$

- For gradient descent, we have (by notation $k_n^l(\theta) = k(\theta, \theta_n^l)$)

$$Q_l(\theta_n^l) = -D\mathcal{J}_l[\mathbf{0}](\theta_n^l) = \mathbb{E}_{\pi_l}\left[\nabla_\theta \log(\pi_y(\theta))k_n^l(\theta) + \nabla_\theta k_n^l(\theta)\right]$$

- Sample average approximation (SAA): $\theta_m^l \sim \pi_l$, $m = 1, \ldots, N$

$$Q_l(\theta_n^l) \approx \frac{1}{N}\sum_{m=1}^{N} \nabla_\theta \log(\pi_y(\theta_m^l))k_n^l(\theta_m^l) + \nabla_\theta k_n^l(\theta_m^l).$$

- Particle updates by the transport map

$$\theta_n^{l+1} = T_l(\theta_n^l) := \theta_n^l + \alpha_l\, Q_l(\theta_n^l), \quad n = 1, \ldots, N.$$

Stein variational Newton (SVN) [Detommaso et al., 2018]

- We seek $Q_l \in \mathcal{T}_N^l = (\mathcal{H}_N^l)^d$, where $\mathcal{H}_N^l = \text{span}(k_1^l(\theta), \ldots, k_N^l(\theta))$,

$$Q_l(\theta) = \sum_{n=1}^{N} c_n^l k_n^l(\theta),$$

where the coefficients $c_n^l \in \mathbb{R}^d$, with $\boldsymbol{c}^l = (c_1^l, \ldots, c_N^l) \in \mathbb{R}^{dN}$.

- For the Newton system: find $Q_l \in \mathcal{T}_N^l$ such that

$$D^2\mathcal{J}_l[\mathbf{0}](V, Q_l) = -D\mathcal{J}_l[\mathbf{0}](V), \quad \forall\, V \in \mathcal{T}_N^l,$$

which, by using the reproducing property, becomes

$$\mathbb{H}\boldsymbol{c}^l = -\boldsymbol{g}^l,$$

gradient: $\boldsymbol{g}^l = (g_1^l, \ldots, g_N^l) \in \mathbb{R}^{dN}$, Hessian: $\mathbb{H} \in \mathbb{R}^{dN \times dN}$.

Stein variational Newton (SVN) [Detommaso et al., 2018]

- The gradient $\boldsymbol{g}^l = (g_1^l, \ldots, g_N^l) \in \mathbb{R}^{dN}$, with $g_m^l \in \mathbb{R}^d$ given by

$$g_m^l = -\frac{1}{N}\sum_{i=1}^{N} \nabla_\theta \log(\pi_y(\theta_i^l)) k_m^l(\theta_i^l) + \nabla_\theta k_m^l(\theta_i^l)$$

- The Hessian $\mathbb{H} \in \mathbb{R}^{dN\times dN}$: with $\mathbb{H}_{mn} \in \mathbb{R}^{d\times d}$ given by

$$\mathbb{H}_{mn} = \frac{1}{N}\sum_{i=1}^{N} -\nabla_\theta^2 \log(\pi_y(\theta_i^l)) k_m^l(\theta_i^l) k_n^l(\theta_i^l) + \nabla_\theta k_m^l(\theta_i^l)(\nabla_\theta k_n^l(\theta_i^l))^\top.$$

- Decouple $dN \times dN$ system to N systems of size $d \times d$

$$\bar{\mathbb{H}}_m c_m^l = -g_m^l, \quad m = 1, \ldots, N,$$

with diagonal approximation (alternative — "mass lumping")

$$\bar{\mathbb{H}}_m = \frac{1}{N}\sum_{i=1}^{N} -\nabla_\theta^2 \log(\pi_y(\theta_i^l)) k_m^l(\theta_i^l) k_m^l(\theta_i^l) + \nabla_\theta k_m^l(\theta_i^l)(\nabla_\theta k_m^l(\theta_i^l))^\top.$$

SVGD vs SVN with $\mathbb{M} = \mathbb{I}$ vs $\mathbb{M} = \bar{\mathbb{H}}$

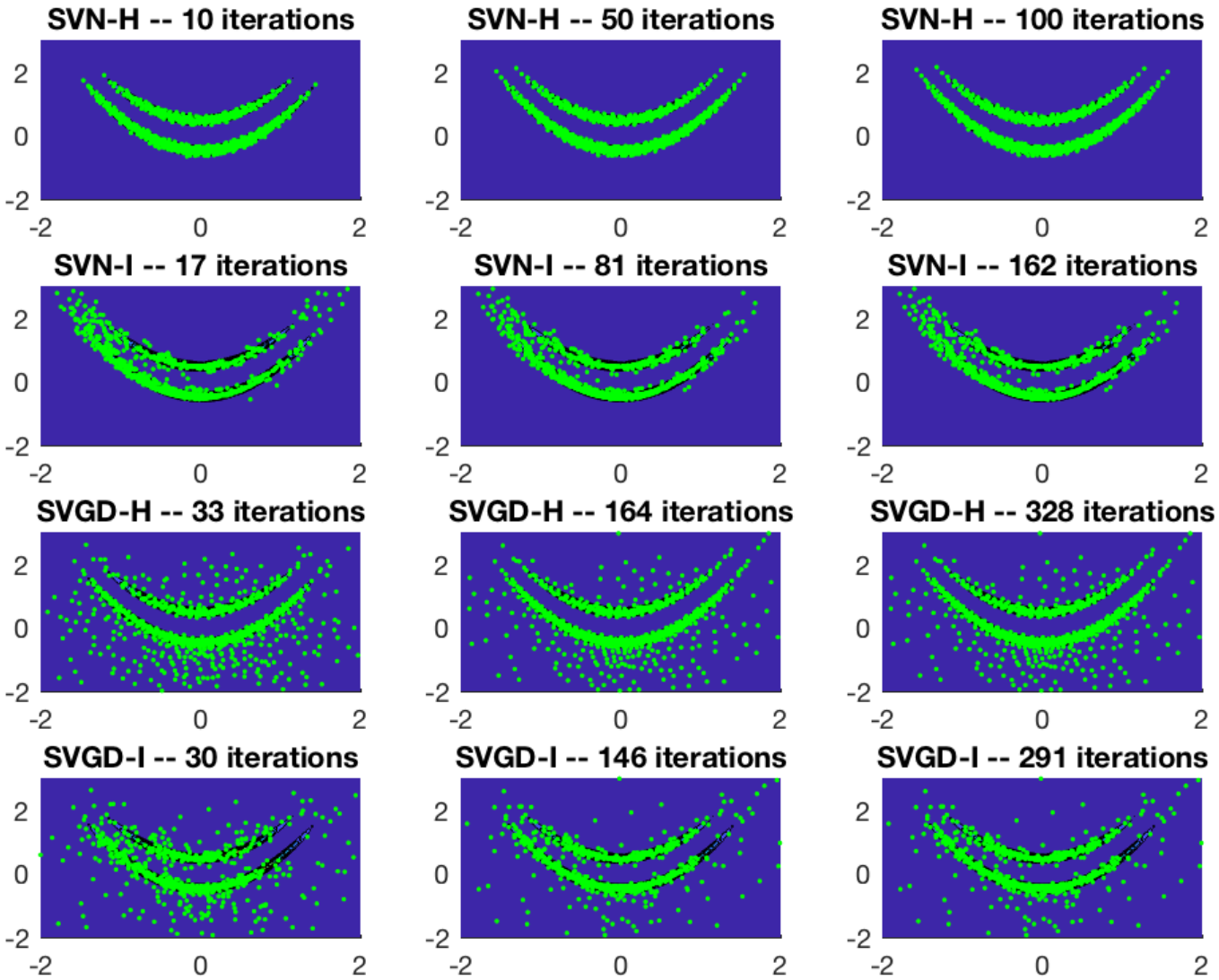

G. Detommaso, T. Cui, Y. Marzouk, A. Spantini, R. Scheichl. A Stein variational Newton method. NeurIPS, 2018.

Outline

Computational challenges in high dimensions

Curse of dimensionality: $d \gg 1$

The number N of basis functions grows rapidly (exponentially) w.r.t. the dimension d to achieve map representation with required accuracy.

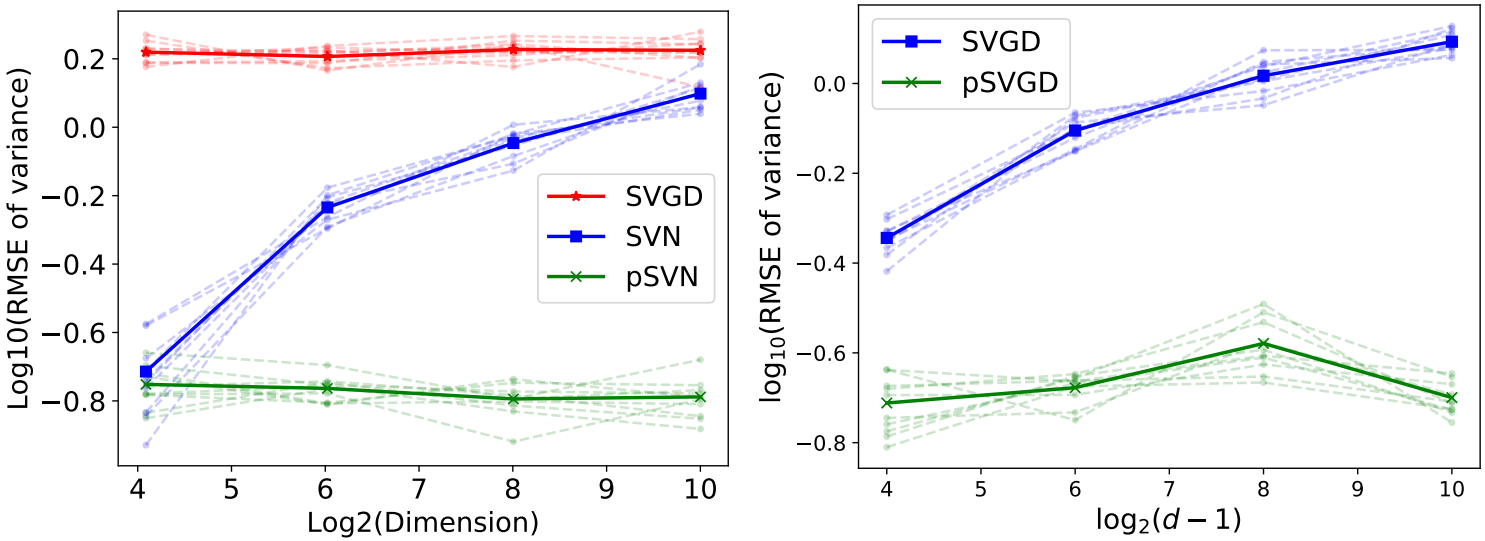

P. Chen, K. Wu, J. Chen, T. O'Leary-Roseberry, O. Ghattas. Projected Stein variational Newton: A fast and scalable Bayesian inference method in high dimensions. NeurIPS, 2019.

P. Chen, O. Ghattas. Projected Stein variational gradient descent. arXiv:2002.03469, 2020.

Intrinsic low dimensionality

The posterior $\neq$ the prior in a low-dimensional subspace.

- high correlation in different dimensions;
- forward map is smoothing/regularizing;
- parameters are anistropic, e.g., Karhunen–Loève expansion.

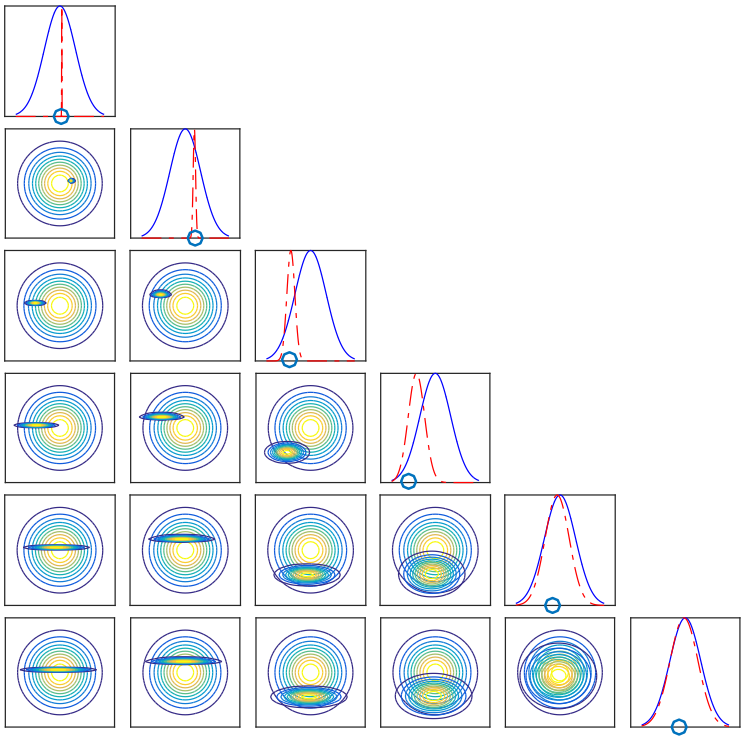

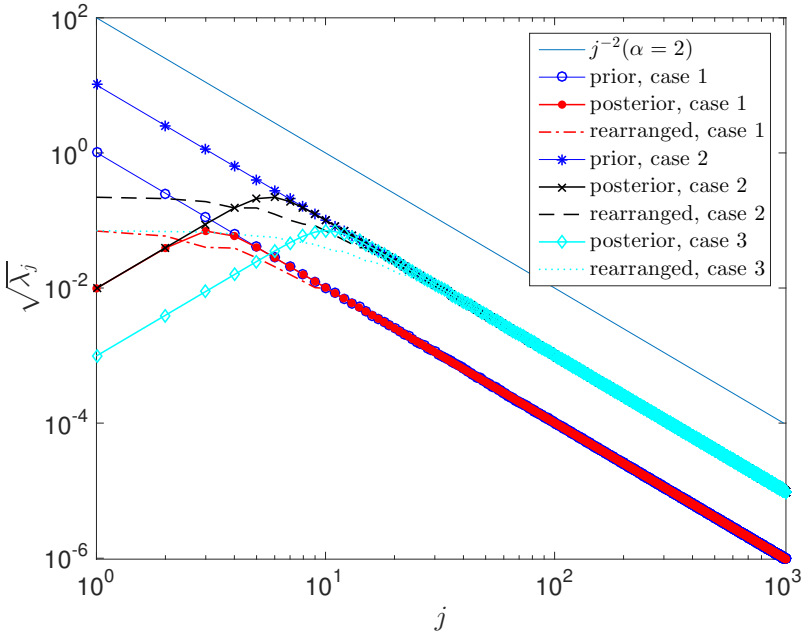

P. Chen, U. Villa, O. Ghattas. Hessian-based adaptive sparse quadrature for infinite-dimensional Bayesian inverse problems. CMAME, 2017.

Projection

- We denote a basis of the subspace of dimension $r < d$ as

$$\Psi = (\psi_1, \ldots, \psi_r) \in \mathbb{R}^{d \times r}, \quad \text{and } \Psi_\perp = (\psi_{r+1}, \ldots, \psi_d) \in \mathbb{R}^{d \times (d-r)}.$$

- We project θ to the low-dimensional subspace as

$$\theta^r = \sum_{i=1}^{r} \psi_i \psi_i^\top \theta = \Psi w.$$

- As a result, we consider the projected posterior

$$\pi_y^r(\theta) = \frac{1}{\pi^r(y)} \, \pi_r(y|\theta^r) \, \pi_0(\theta), \tag{2}$$

with profile function $\pi_r(y|\theta^r)$, where the normalization constant

$$\pi^r(y) = \mathbb{E}_{\pi_0}[\pi_r(y|\theta^r)].$$

Optimal profile function

- We decompose the prior density for $w \in \mathbb{R}^r$ and $v_\perp \in \mathbb{R}^{d-r}$

$$\pi_0(\Psi w + \Psi_\perp v_\perp) = \pi_0^r(w)\pi_0^\perp(v_\perp|w),$$

- where the marginal density

$$\pi_0^r(w) = \int_{R^{d-r}} \pi_0(\Psi w + \Psi_\perp v_\perp) dv_\perp,$$

- and the conditional density

$$\pi_0^\perp(v_\perp|w) = \pi_0(\Psi w + \Psi_\perp v_\perp)/\pi_0^r(w).$$

- We define the profile function π_r^* as

$$\pi_r^*(y|\theta^r) = \int_{\mathbb{R}^{d-r}} \pi(y|(\theta^r + \Psi_\perp v_\perp))\pi_0^\perp(v_\perp|w) dv_\perp.$$

- Optimal projected posterior [Zahm et. al., 2019]

$$\mathcal{D}_{\mathsf{KL}}(\pi_y|\pi_y^{r,*}) \leq \mathcal{D}_{\mathsf{KL}}(\pi_y|\pi_y^r).$$

Basis construction

The basis functions Ψ for projection are obtained by

$$H\psi_i = \lambda_i C_0^{-1}\psi_i, \quad i = 1, \ldots, r,$$

which corresponds to the r largest (in $|\cdot|$) eigenvalues, i.e., $|\lambda_1| \geq \cdots \geq |\lambda_r|$. C_0: prior covariance. With $\eta_y(\theta) = -\log(\pi(y|\theta))$

- **Gradient-based subspace:**

$$H = \mathbb{E}_\pi \left[\nabla_\theta \eta_y(\theta) (\nabla_\theta \eta_y(\theta))^\top \right].$$

- **Hessian-based subspace:**

$$H = \mathbb{E}_\pi \left[\nabla_\theta^2 \eta_y(\theta) \right].$$

- **Choice of the density π:** density at step l, i.e., π_l.

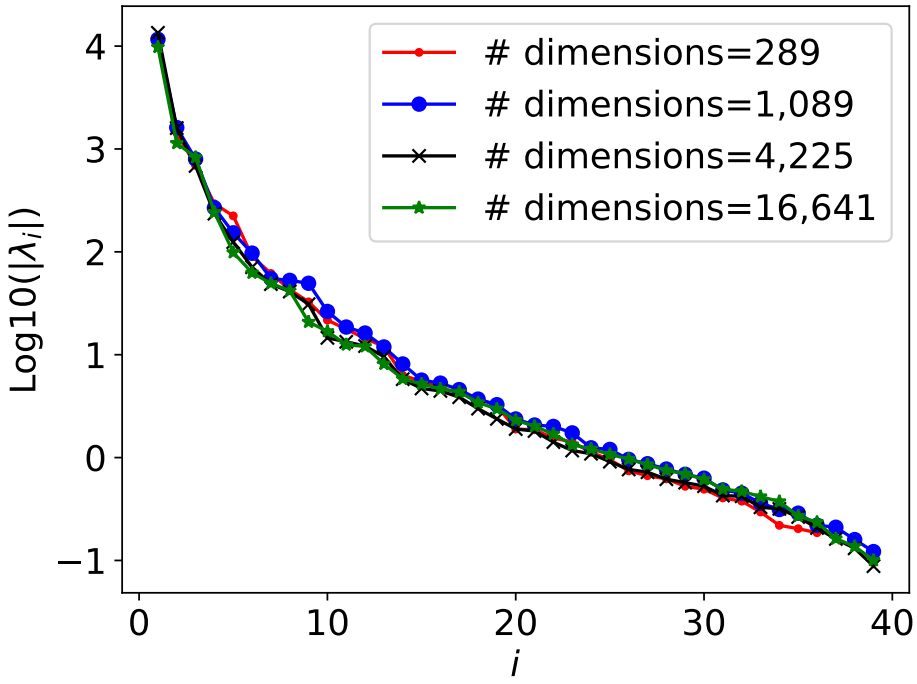

Error estimates – Hessian based projection

Assumption

Assume that the parameter-to-observable map $\mathcal{O}$ satisfies:

1. *There exists a constant $C_{\mathcal{O}} > 0$ such that $\mathbb{E}_{\pi_0}[||\mathcal{O}(\cdot)||_\Gamma] \leq C_{\mathcal{O}}$.*
2. *For every $b > 0$, there exists a constant $C_b > 0$ such that*

$$||\mathcal{O}(\theta_1) - \mathcal{O}(\theta_2)||_\Gamma \leq C_b||\theta_1 - \theta_2||_\Theta, \quad \text{for } \max\{||\theta_1||_\Theta, ||\theta_2||_\Theta\} < b.$$

Theorem

For Hessian-based projection, there holds

$$\mathcal{D}_{KL}(\pi_y \,|\, \pi_y^r) \leq C||\theta - \theta^r||_\Theta,$$

C independent of d, r.

Error estimates – gradient based projection

Assumption

Assume that the prior density $\pi_0(\theta) \propto \exp(-V(\theta) - W(\theta))$ *such that*

1. $V \in C^2(\mathbb{R}^d)$, *and there exists a s.p.d.* $\Gamma \in \mathbb{R}^{d\times d}$ *such that*

$$z^T \nabla^2 V(\theta) z \geq z^T \Gamma z \quad \forall z \in \mathbb{R}^d, \theta \in \mathbb{R}^d.$$

2. W *is bounded in* $\mathbb{R}^d$.

Theorem

For gradient-based projection, using [Zahm et. al., 2019], there holds

$$\mathcal{D}_{KL}(\pi_y \,|\, \pi_y^r) \leq C \sum_{i=r+1}^{d} \lambda_i,$$

C independent of d.

Projected Stein variational methods

- By decomposition $\theta = \theta^r + \theta^\perp$, we have

$$\pi_y^r(\theta) = \pi_r(y|\theta^r)\ \pi_0^r(\theta^r)\ \pi_0^\perp(\theta^\perp|\theta^r).$$

- With $\theta^\perp$ frozen, by $\theta^r = \Psi w$, we define

$$p_0(w) := \pi_0^r(\theta^r), \quad p_y(w) := \pi_y^r(\theta^r) = \pi_r(y|\theta^r)\pi_0^r(\theta^r).$$

- We seek $T = T_L \circ T_{L-1} \circ \cdots \circ T_1 \circ T_0 : \mathbb{R}^r \to \mathbb{R}^r$, such that

$$\min_{T \in \mathcal{T}} D_{KL}(T_\sharp p_0 | p_y).$$

- Apply **SVGD/SVN** in $\mathbb{R}^r$ for w, **pSVGD/pSVN** where

$$\nabla_w \log(p_y(w)) = \Psi^\top \nabla_\theta \log(\pi_y^r(\theta^r)),$$

and

$$\nabla_w^2 \log(p_y(w)) = \Psi^\top \nabla_\theta^2 \log(\pi_y^r(\theta^r))\Psi.$$

Algorithm 1 pSVGD in parallel using MPI

Input: N prior samples, $\theta_1^0, \ldots, \theta_N^0$, in each of K cores, Ψ.
Output: posterior samples $\theta_1^y, \ldots, \theta_N^y$ in each core.
Perform projection to get $\theta_n = \theta_n^r + \theta_n^\perp$ and the samples w_n^{l-1}.
Perform MPI_Allgather for w_n^{l-1}, $n = 1, \ldots, M$.
repeat
    Compute the gradient of the log-posterior.
    Perform MPI_Allgather for the gradient.
    Compute the kernel and its gradient.
    Update the samples $w_1^l, \ldots, w_N^l$.
    Perform MPI_Allgather for w_n^l, $n = 1, \ldots, N$.
    Update the samples $\theta_n^r = \Psi w_n^l$, $n = 1, \ldots, N$.
    Set $l \leftarrow l + 1$.
until A stopping criterion is met.
Reconstruct samples $\theta_n^y = \theta_n^r + \theta_n^\perp$, $n = 1, \ldots, N$.

Algorithm 2 Adaptive pSVGD

1: **Input**: N prior samples, $\theta_1^0, \ldots, \theta_N^0$, in each of K cores.
2: **Output**: posterior samples $\theta_1^y, \ldots, \theta_N^y$ in each core.
3: Set level $l_2 = 1$, $\theta_n^{l_2-1} = \theta_n^0$, $n = 1, \ldots, N$.
4: **repeat**
5: Perform the eigendecomposition and form the bases Ψ^{l_2}.
6: Apply **Algorithm** pSVGD to update the samples $[\theta_1^{l_2}, \ldots, \theta_N^{l_2}] = \text{pSVGD}([\theta_1^{l_2-1}, \ldots, \theta_N^{l_2-1}], K, \Psi^{l_2})$.
7: Set $l_2 \leftarrow l_2 + 1$.
8: **until** A stopping criterion is met.

Advantages:

- Avoids/alleviates the curse of dimensionality.
- Largely reduces computational cost with $r \ll d$.
- Converges faster in low-dimensional space.
- Parallel computation with reduced communication.

pSVGD: Accuracy

We consider a nonlinear Bayesian inverse problem with

$$\mathcal{O}(\theta) = O(S(\theta)), \quad u = S(\theta), \quad -\nabla \cdot (e^{\theta} \nabla u) = 0, \text{ in } (0,1)^2$$

Gaussian prior $\mathcal{N}(0, C_0)$, where C_0 is a discretization of $(I - 0.1\triangle)^{-2}$. We test the accuracy using a dimension-independent likelihood informed (DILI) MCMC method with 10,000 samples as reference.

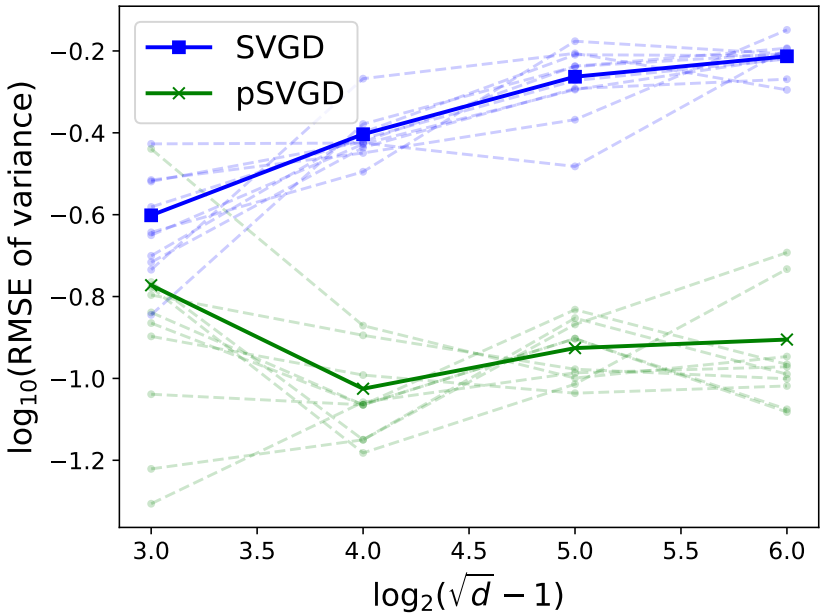

RMSE of pointwise sample variance in L_2-norm, with 256 samples, SVGD and pSVGD both terminated at $\ell = 200$ iterations, parameter dimension $d = (2^n + 1)^2$, with $n = 3, 4, 5, 6$.

pSVGD: Scalability

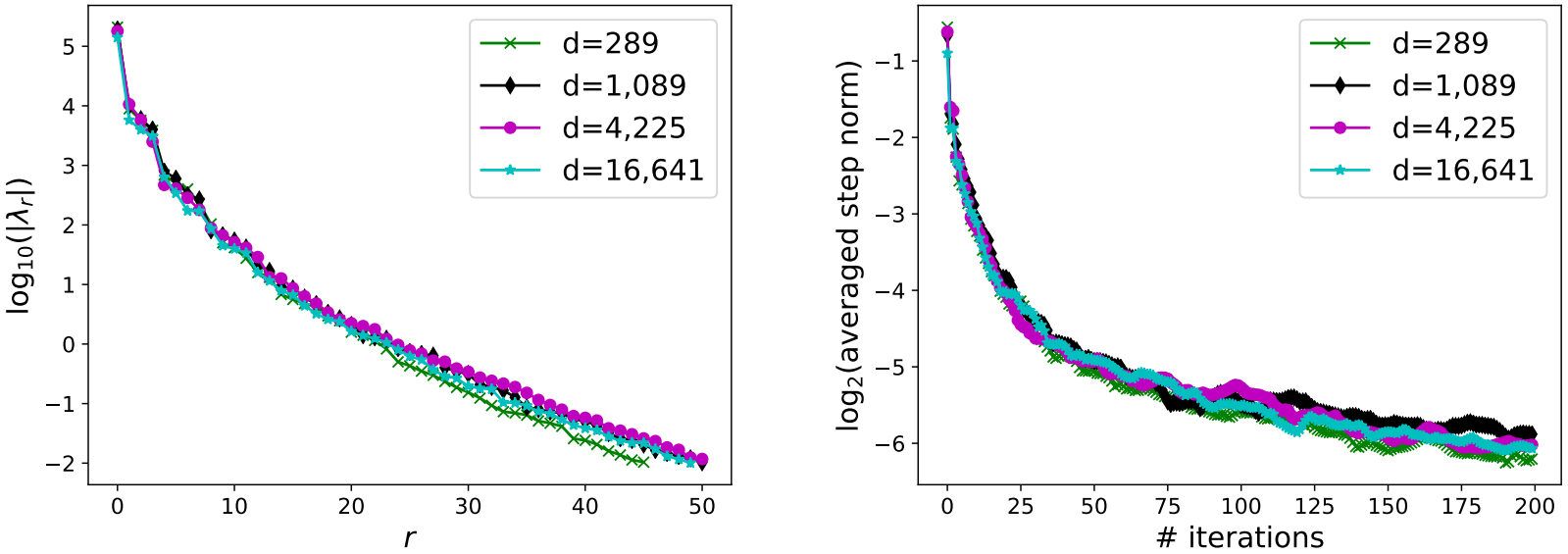

Scalability w.r.t. the parameter dimension d by decay of eigenvalues λ_r w.r.t. r (left), and decay of the averaged step norm $\text{mean}_m ||w_m^{\ell+1} - w_m^{\ell}||_2$ w.r.t. the number of iterations (right).

pSVGD: Scalability

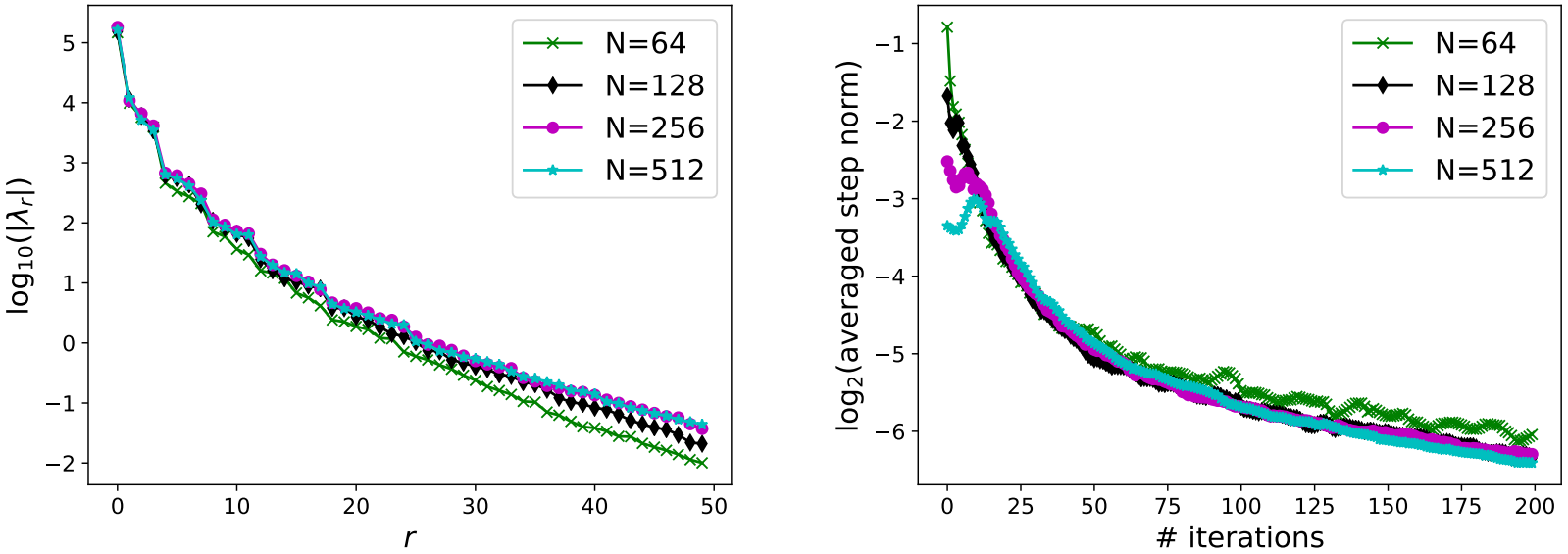

Scalability w.r.t. the number of samples N by decay of eigenvalues λ_r w.r.t. r (left), and decay of the averaged step norm $\text{mean}_m ||w_m^{\ell+1} - w_m^{\ell}||_2$ w.r.t. the number of iterations (right).

pSVGD: Scalability

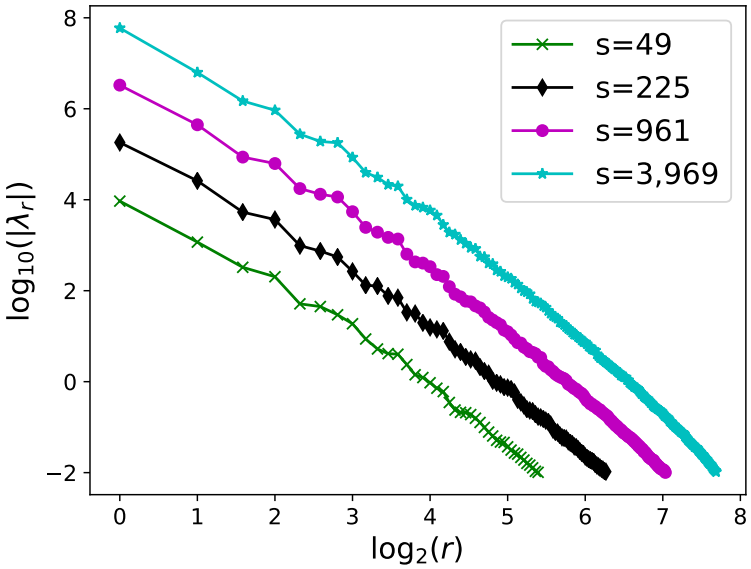

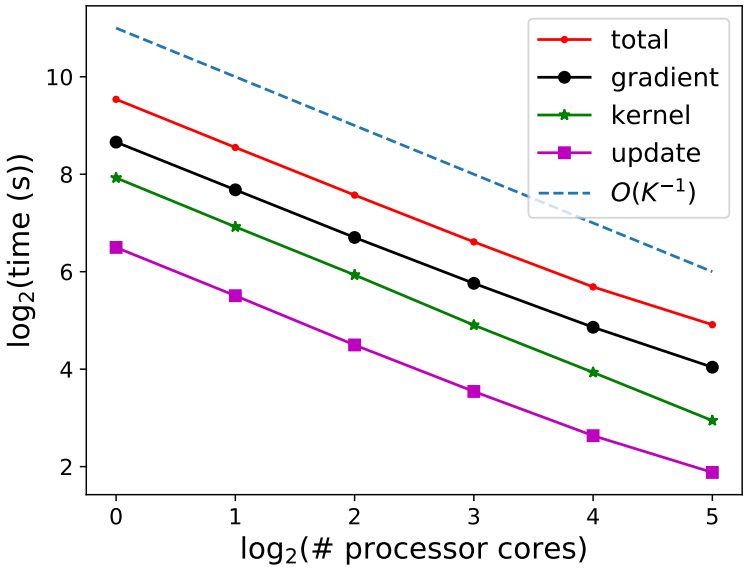

Scalability w.r.t. the number of data points s by decay of eigenvalues λ_r w.r.t. r (top), and the number of processor cores K by decay of CPU time for different parts of pSVGD (bottom).

pSVN: Accuracy

We consider a nonlinear Bayesian inverse problem with

$$\mathcal{O}(\theta) = O(S(\theta)), \quad u = S(\theta), \quad -\nabla \cdot (e^{\theta} \nabla u) = 0, \text{ in } (0,1)^2$$

Gaussian prior $\mathcal{N}(0, C_0)$, where C_0 is a discretization of $(I - 0.1\triangle)^{-2}$. We test the accuracy against a dimension-independent likelihood informed (DILI) MCMC method with 10,000 samples as reference.

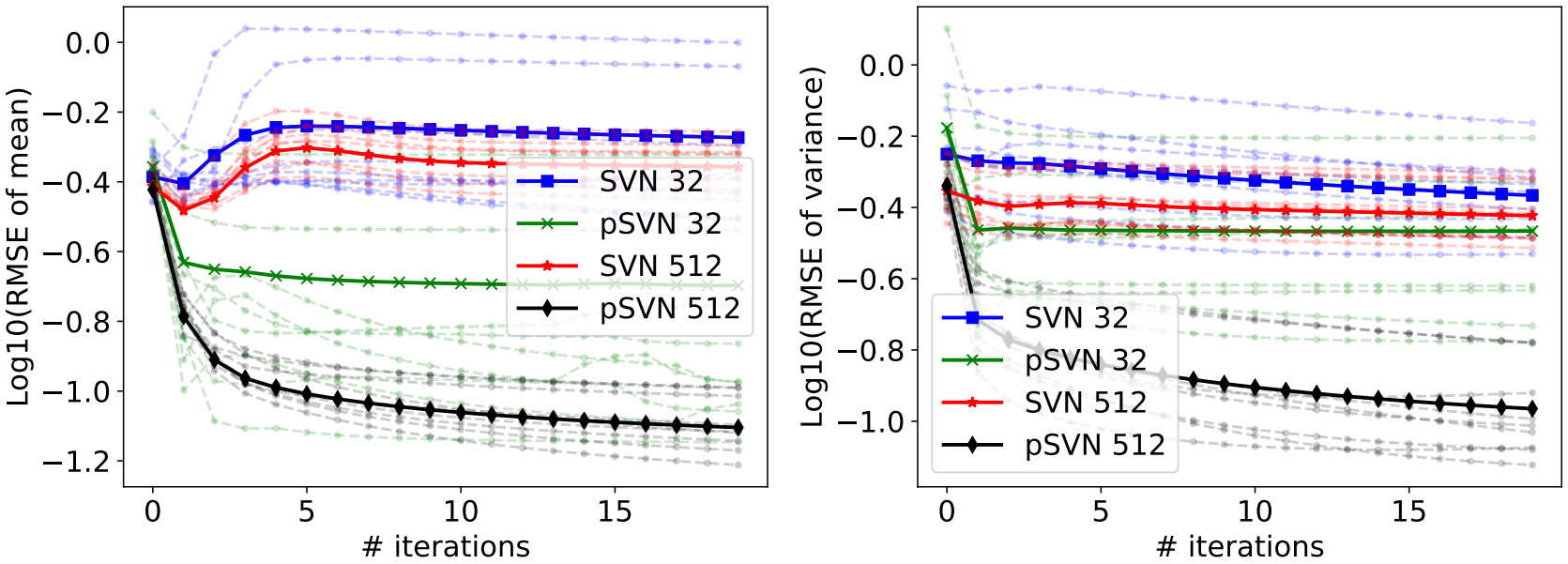

Decay of the RMSE of the L2 of the mean (left) and pointwise variance (right) of the parameter with dimension $d = 1089$ and $N = 32$ and 512 samples.

pSVN: Scalability

We consider a nonlinear Bayesian inverse problem with

$$\mathcal{O}(\theta) = O(S(\theta)), \quad u = S(\theta), \quad -\nabla \cdot (e^{\theta} \nabla u) = 0, \text{ in } (0,1)^2$$

Gaussian prior $\mathcal{N}(0, C_0)$, where C_0 is a discretization of $(I - 0.1\triangle)^{-2}$. We test the accuracy against a dimension-independent likelihood informed (DILI) MCMC method with 10,000 samples as reference.

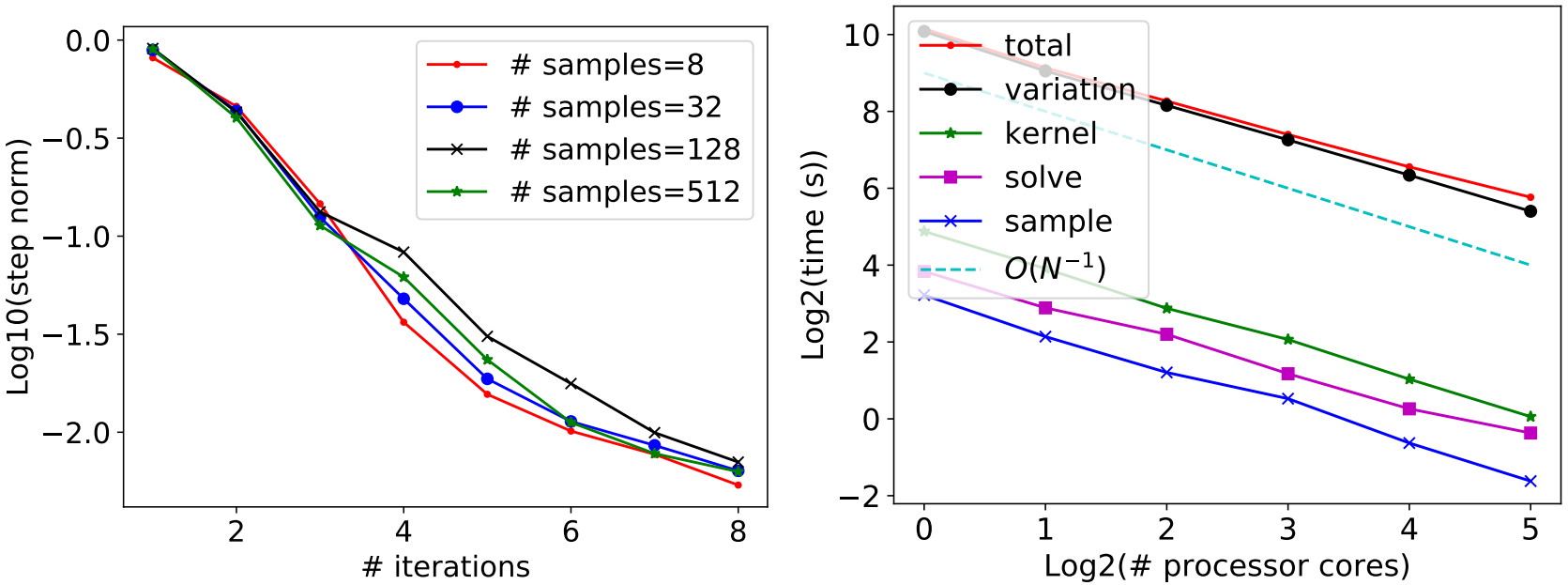

Left: Decay of the averaged norm of the update $w^{l+1} - w^l$ w.r.t. the iteration number l, with increasing number of samples. Right: Decay of the wall clock time of different computational components w.r.t. increasing # cores.

Summary

Take away message: pSVGD/pSVN

- effectively alleviates the curse of dimensionality;
- is scalable w.r.t. # parameters, samples, data points, CPU cores.

Further investigation:

- Correlation and dimension reduction in data space.
- Convergence analysis w.r.t. # parameters, samples.
- Practical applications.

P. Chen, K. Wu, J. Chen, T. O'Leary-Roseberry, O. Ghattas. Projected Stein variational Newton: A fast and scalable Bayesian inference method in high dimensions. NeurIPS, 2019.

P. Chen, O. Ghattas. Projected Stein variational gradient descent. arXiv:2002.03469, 2020.

Outline

PDE-constrained Bayesian inversion

- We have the data model

$$y = \mathcal{B}(u(\theta)) + \xi$$

where u is the solution of the PDE (in weak form)

$$A(u(\theta), v; \theta) = F(v) \quad v \in V$$

$\mathcal{B} : V \to Y$ is a vector of observational functionals.

- Examples: linear diffusion, elasiticity, Stokes flow, acoustic, etc.,

$$-\nabla \cdot (\kappa(\theta)\nabla u) = f, \qquad \text{in } D,$$

with suitable boundary conditions, which leads to

$$A(u, v; \theta) = \int_D \kappa(x, \theta)\nabla u(x, \theta) \cdot \nabla v(x)dx, \; F(v) = \int_D f(x)v(x)dx.$$

- With Gaussian noise $\xi \in \mathcal{N}(0, \Gamma)$, we define the potential

$$\eta_y(\theta) := \frac{1}{2}(y - \mathcal{B}(u(\theta)))^T \Gamma^{-1}(y - \mathcal{B}(u(\theta))) \Rightarrow \pi(y|\theta) = \log(-\eta_y(\theta)).$$

High-fidelity approximation of the potential η_y

E.g. finite element, we consider: find $u_h \in V_h \subset V$ such that

$$A(u_h, v_h, \theta) = F(v_h) \quad \forall v_h \in V_h. \tag{3}$$

Then the data model is given by

$$y = \mathcal{B}(u_h(\theta)) + \xi,$$

then for $\xi \sim \mathcal{N}(0, \Gamma)$ the likelihood function is given by

$$\pi(y|\theta) = \exp(-\eta_y(u_h(\theta))),$$

where the potential $\eta_y(u_h(\theta))$ (nonlinear w.r.t. u_h)

$$\eta_y(u_h(\theta)) = \frac{1}{2}(y - \mathcal{B}(u_h(\theta)))^T \Gamma^{-1}(y - \mathcal{B}(u_h(\theta))).$$

For SVGD, and the projected SVGD, we also need

$$-\nabla_\theta \log(\pi_y(\theta)) = \nabla_\theta \eta_y(u_h(\theta)) + \frac{\nabla_\theta \pi_0(\theta)}{\pi_0(\theta)}.$$

High-fidelity approximation of the gradient $\nabla_\theta \eta_y$

We form a Lagrangian

$$L(u_h, p_h, \theta) = \eta_y(u_h) + A(u_h, p_h, \theta) - F(p_h),$$

$\partial_v L w_h = 0$ to obtain the adjoint p_h, i.e., find $p_h \in V$ such that

$$A(w_h, p_h; \theta) = -\partial_u \eta_y|_{u_h}(w_h) \quad \forall w_h \in V_h, \tag{4}$$

where

$$\partial_u \eta_y|_{u_h}(w_h) = -\mathcal{B}(w_h)^T \Gamma^{-1}(y - \mathcal{B}(u_h)).$$

Then the gradient is given by

$$\nabla_\theta \eta_y(u_h(\theta)) = \partial_\theta L(u_h, p_h; \theta) = \partial_\theta A(u_h, p_h, \theta).$$

Model reduction

High-fidelity approximation

Finite element space V_h,

$$\dim(V_h) = N_h$$

Given θ, find $u_h \in V_h$ s.t.

$$A(u_h, v_h; \theta) = F(v_h) \ \forall v_h \in V_h$$

The algebraic system is

$$\mathbb{A}_h(\theta)\boldsymbol{u}_h = \boldsymbol{f}_h$$

$$\mathbb{V} = [\boldsymbol{\psi}_1, \ldots, \boldsymbol{\psi}_N]$$

$$\mathbb{V}^T \boldsymbol{u}_h = \boldsymbol{u}_N$$

$$\mathbb{V}^T \mathbb{A}_h(\theta)\mathbb{V} = \mathbb{A}_N(\theta)$$

$$\mathbb{V}^T \boldsymbol{f}_h = \boldsymbol{f}_N$$

Reduced basis approximation

Reduced basis space $V_N \subset V_h$,

$$\dim(V_N) = N$$

Given θ, find $u_N \in V_N$ s.t.

$$A(u_N, v_N; \theta) = F(v_N) \ \forall v_N \in V_N$$

The algebraic system is

$$\mathbb{A}_N(\theta)\boldsymbol{u}_N = \boldsymbol{f}_N$$

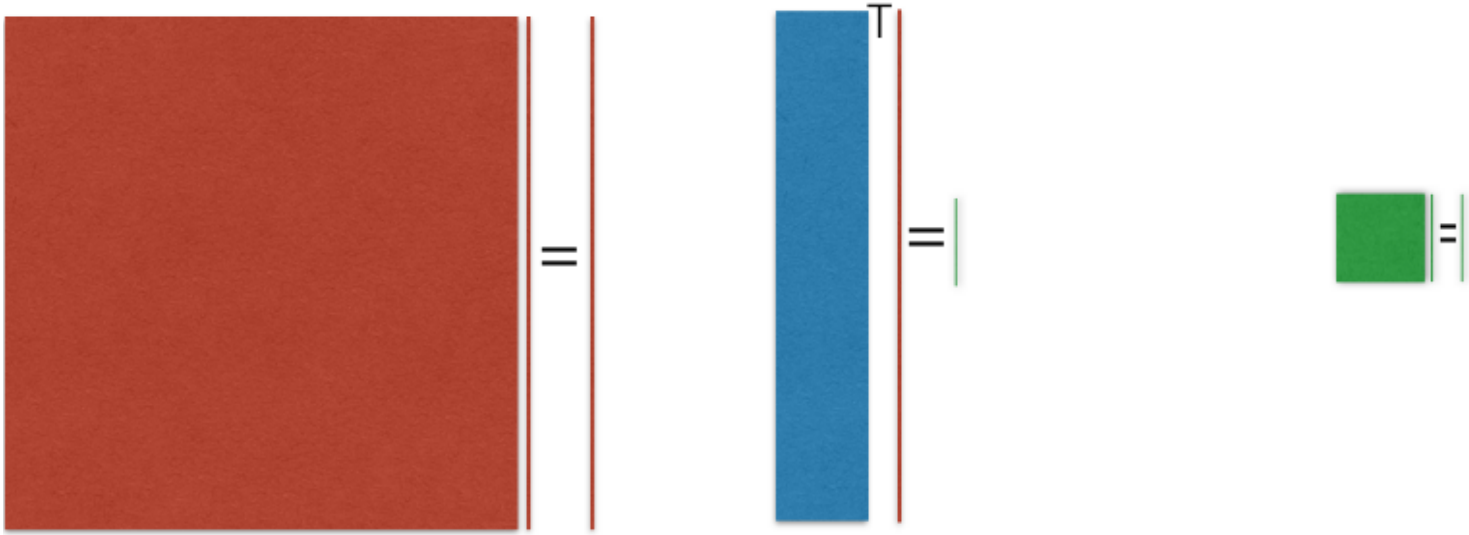

Model reduction: Building blocks

POD/SVD

Training samples

$$\Xi_t = \{\theta^n, n = 1, \ldots, N_t\}$$

Compute snapshots

$$\mathbb{U} = [\boldsymbol{u}_h(\theta^1), \ldots, \boldsymbol{u}_h(\theta^{N_t})]$$

Perform SVD

$$\mathbb{U} = \mathbb{V}\Sigma\mathbb{W}^T$$

Extract bases $\mathbb{V}[1:N,:]$

$$N = \text{argmin}_n \, \mathcal{E}_n(\Sigma) \geq 1 - \varepsilon$$

Greedy algorithm

Training samples

$$\Xi_t = \{\theta^n, n = 1, \ldots, N_t\}$$

Initialize V_N for $N = 1$ as

$$V_N = \text{span}\{u_h(\theta^1)\}$$

Pick next sample such that

$$\theta^{N+1} = \text{argmax}_{\theta \in \Xi_t} \Delta_N(\theta)$$

Update bases V_{N+1} as

$$V_N \oplus \text{span}\{u_h(\theta^{N+1})\}$$

Offline-Online

Affine assumption/approx.

$$A = \sum_{q=1}^{Q} \theta_q(\theta) A_q$$

Offline computation once

$$\mathbb{A}_N^q = \mathbb{V}^T \mathbb{A}_h^q \mathbb{V}$$

Online assemble

$$\mathbb{A}_N(\theta) = \sum_{q=1}^{Q} \theta_q(\theta) \mathbb{A}_N^q$$

Online solve

$$\mathbb{A}_N(\theta)\boldsymbol{u}_N = \boldsymbol{f}_N$$

Goal-oriented a-posteriori error estimate $\Delta_N(\theta)$ – dual weighted residual

$$\Delta_N(\theta) = A(u_N, p_N, \theta) - F(p_N)$$

Reduced basis approximation of the potential η_y

RB approximation for the adjoint problem: find $p_N \in W_N$ s.t.

$$A(w_N, p_N, \theta) = -\partial_u \eta_y|_{u_N}(w_N) \quad \forall w_N \in W_N.$$

The goal-oriented a-posterior error estimate is given by

$$\Delta_N(\theta) = A(u_N, p_N, \theta) - F(p_N).$$

RB approximation for the potential $\eta_y(\theta)$:

$$\eta_{y,N}(\theta) = \eta_y(u_N(\theta)).$$

Dual-weighted residual correction:

$$\eta_{y,N}^{\Delta}(\theta) = \eta_{y,N}(\theta) + \Delta_N(\theta).$$

Reduced basis approximation of the gradient $\nabla_\theta \eta_y$

With the RB state u_N and adjoint p_N, the gradient is given by

$$\nabla_\theta \eta_y(u_N(\theta)) = \partial_\theta A(u_N, p_N; \theta).$$

For the modified potential $\eta_{y,N}^\Delta(\theta)$, we form the Lagrangian

$$\begin{aligned} L(u_N, p_N, \hat{u}_N, \hat{p}_N; \theta) = \eta_{y,N}^\Delta(\theta) + A(u_N, \hat{u}_N; \theta) - F(\hat{u}_N) \\ + A(\hat{p}_N, p_N; \theta) + \nabla_u \eta_y|_{u_N}(\hat{p}_N), \end{aligned}$$

and solve the variational problem: find $\hat{p}_N \in W_N$

$$A(\hat{p}_N, w_N; \theta) = F(w_N) - A(u_N, w_N; \theta), \quad \forall w_N \in W_N,$$

and the variational problem: find $\hat{u}_N \in V_N$

$$A(v_N, \hat{u}_N; \theta) = -A(v_N, p_N; \theta) - \partial_u \eta_y|_{u_N}(v_N) - \nabla_u^2 \eta_y|_{u_N}(\hat{p}_N, v_N), \ \forall v_N \in V_N,$$

which leads to the gradient

$$\nabla_\theta \eta_{y,N}^\Delta(\theta) = \partial_\theta L(u_N, p_N, \hat{u}_N, \hat{p}_N; \theta).$$

Error estimates for the state and adjoint

Assumption: Well-posedness

The bilinear form $A(\cdot,\cdot;\theta) : V \times V \to \mathbb{R}$ and linear form $F(\cdot) : V \to \mathbb{R}$ satisfy

A1 At any $\theta \in \Theta$, there exist a coercivity constant $\alpha(\theta) > 0$ and a continuity constant $\gamma(\theta) > 0$ such that

$$\alpha(\theta)||w||_V^2 \leq A(w,w;\theta) \text{ and } A(w,v;\theta) \leq \gamma(\theta)||w||_V||v||_V, \ \forall w,v \in V.$$

The linear functional $F(\cdot) : V \to \mathbb{R}$ is bounded with norm

$$||F(\cdot)||_{V'} < \infty.$$

A2 Moreover, $A(\cdot,\cdot;\theta)$ is continuously differentiable w.r.t. θ at every $\theta \in \Theta$, and for each $j = 1,\ldots,d$, there exists $\rho_j(\theta) < \infty$ such that

$$\partial_{\theta_j} A(w,v;\theta) \leq \rho_j(\theta)||w||_V||v||_V, \ \forall w,v \in V.$$

Error estimates for the state u and adjoint p

Let $e_r^u(\theta)$ and $e_r^p(\theta)$ denote the RB state and adjoint errors

$$e_r^u(\theta) := u_h(\theta) - u_N(\theta), \quad e_r^p(\theta) := p_h(\theta) - p_N(\theta).$$

Let $R_u(u_N, \cdot; \theta)$ denotes the residual of the state equation

$$R_u(u_N, v_h; \theta) = A(u_N, v_h; \theta) - F(v_h; \theta) \quad \forall v_h \in V_h,$$

and $R_p(p_N, \cdot; \theta)$ denotes the residual of the adjoint equation

$$R_p(w_h, p_N; \theta) = A(w_h, p_N; \theta) + \nabla_u \eta_y|_{u_N}(w_h) \quad \forall w_h \in V_h.$$

Lemma: Error estimates for the state u and adjoint p

Under the well-posedness assumption, for any $\theta \in \Theta$, there holds

$$||e_r^u(\theta)||_V \leq \frac{1}{\alpha(\theta)} ||R_u(u_N, \cdot; \theta)||_{V'},$$

and

$$||e_r^p(\theta)||_V \leq \frac{1}{\alpha(\theta)} ||R_p(\cdot, p_N; \theta)||_{V'} + \frac{C_{\mathcal{O}}}{\alpha(\theta)} ||e_r^u(\theta)||_V.$$

Error estimates for the potential η_y and gradient $\nabla_\theta \eta_y$

Lemma: Error esstimates for $\eta_{y,N}(\theta)$ and $\eta^{\Delta}_{y,N}(\theta)$.

There exists constant $C(\theta) > 0$ for each $\theta \in \Theta$, independent of N, s.t.

$$|e^{\eta}_r(\theta)| := |\eta_y(\theta) - \eta_{y,N}(\theta)| \leq C(\theta)||e^u_r(\theta)||_V.$$

There exists constant $C_1(\theta) > 0$ for each $\theta \in \Theta$, independent of N, s.t.

$$|e^{\Delta}_r(\theta)| := |\eta_y(\theta) - \eta^{\Delta}_{y,N}(\theta)| \leq C||e^u_r(\theta)||_V(||e^u_r(\theta)||_V + ||e^p_r(\theta)||_V).$$

Lemma: Error esstimates for $\nabla_\theta \eta_{y,N}(\theta)$ and $\nabla_\theta \eta^{\Delta}_{y,N}(\theta)$

There exist $C_1(\theta), C_2(\theta) > 0$ for each $\theta \in \Theta$, independent of N, s.t.

$$||\nabla_\theta e^{\eta}_r(\theta)||_1 \leq C_1(\theta)||\nabla_\theta e^u_r(\theta)||_{V^d} + C_2(\theta)||\nabla_\theta u_N(\theta)||_{V^d}||e^u_r(\theta)||_V.$$

There exist $C_1(\theta), , C_2(\theta), C_3(\theta), C_4(\theta) > 0$, independent of N, such that

$$\begin{aligned}||\nabla_\theta e^{\Delta}_r(\theta)||_1 \leq\ & C_1||\nabla_\theta e^u_r(\theta)||_{V^d}||e^p_r(\theta)||_V + C_2||\nabla_\theta e^p_r(\theta)||_{V^d}||e^u_r(\theta)||_V \\ & + C_3||e^u_r(\theta)||_V||e^p_r(\theta)||_V + C_4||\nabla_\theta e^u_r(\theta)||_{V^d}||e^u_r(\theta)||_V.\end{aligned}$$

Error estimates for the posterior π_y

Theorem: Error estimates for the posterior π_y

$$D_{\mathrm{KL}}(\pi_y^h|\pi_y^r) \leq \mathbb{E}_{\pi_y^h}\left[|e_r^\eta|\right] + \mathbb{E}_{\pi_y^h}[|\exp(e_r^\eta) - 1|],$$

and

$$D_{\mathrm{KL}}(\pi_y^h|\pi_y^\Delta) \leq \mathbb{E}_{\pi_y^h}\left[|e_r^\Delta|\right] + \mathbb{E}_{\pi_y^h}[|\exp(e_r^\Delta) - 1|].$$

Corollary: Error estimates for the posterior π_y

Let $\Theta_1 =: \{\theta \in \Theta : e_r^\eta(\theta) < 1\}$, if

$$\mathbb{E}_{\pi_y^h(\Theta\setminus\Theta_1)}[|\exp(e_r^\eta) - 1|] < \delta\mathbb{E}_{\pi_y^h}\left[|e_r^\eta|\right]$$

for some constant $\delta > 0$, we have

$$D_{\mathrm{KL}}(\pi_y^h|\pi_y^r) \leq (3+\delta)\mathbb{E}_{\pi_y^h}\left[|e_r^\eta|\right].$$

The same holds for $D_{\mathrm{KL}}(\pi_y^h|\pi_y^\Delta) \leq (3+\delta)\mathbb{E}_{\pi_y^h}\left[|e_r^\Delta|\right]$.

Algorithm 3 Adaptive greedy algorithm with Stein samples

Input: samples $\theta_m^0 \sim \pi_0$, $m = 1, \ldots, M$, tolerance ε_r^0, update step k.
Output: Stein samples θ_m, $m = 1, \ldots, M$.
Initialization: at $\theta = \theta_1^0$, solve the high-fidelity state and adjoint problems for u_h and p_h, set $V_r = \text{span}\{u_h\}$ and $W_r = \text{span}\{p_h\}$, compute the reduced matrices and vectors for once.
while at step $l = 0, k, 2k, \ldots,$ of the SVGD algorithm **do**
    Compute the error indicator $\triangle_N(\theta_m^l)$ for $m = 1, \ldots, M$.
    while $\max_{m=1,\ldots,M} |\triangle_N(\theta_m^l)| > \varepsilon_r^l$ **do**
        Choose $\theta = \text{argmax}_{\theta_m^l, m=1,\ldots,M} |\triangle_N(x_m^l)|$.
        Solve the high-fidelity problems for u_h and p_h at θ.
        Enrich the spaces $V_r = V_r \bigoplus \text{span}\{u_h\}$, $W_r = W_r \bigoplus \text{span}\{p_h\}$.
        Compute all the reduced matrices and vectors for once.
        Compute the error indicator $\triangle_N(\theta_m^l)$ for $m = 1, \ldots, M$.
    end while
    Perform SVGD update with RB approximations.
    Update the tolerance ε_r^l according to gradient in SVGD algorithm.
end while

Numerical example

We consider the diffusion problem

$$-\nabla \cdot (a(\theta, x)\nabla u) = f(x), \quad x \in D = (0,1)^2,$$

where $f = 1$, the coefficient

$$a(\theta, x) = 5 + \sum_{1 \le i+j \le 4} \frac{1}{\sqrt{i^2 + j^2}} \theta_{i,j} \cos(i\pi x_1) \cos(j\pi x_2).$$

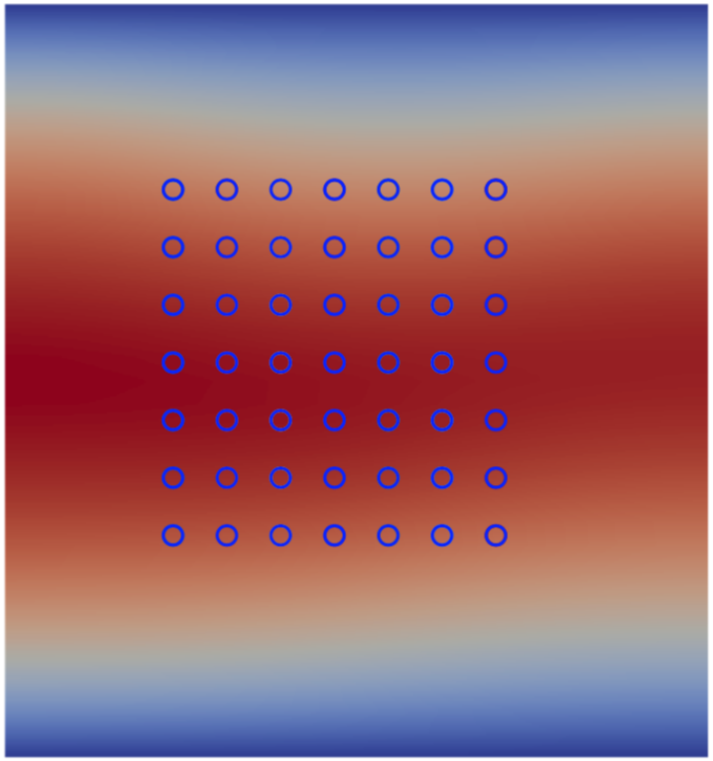

Numerical results: Comparison

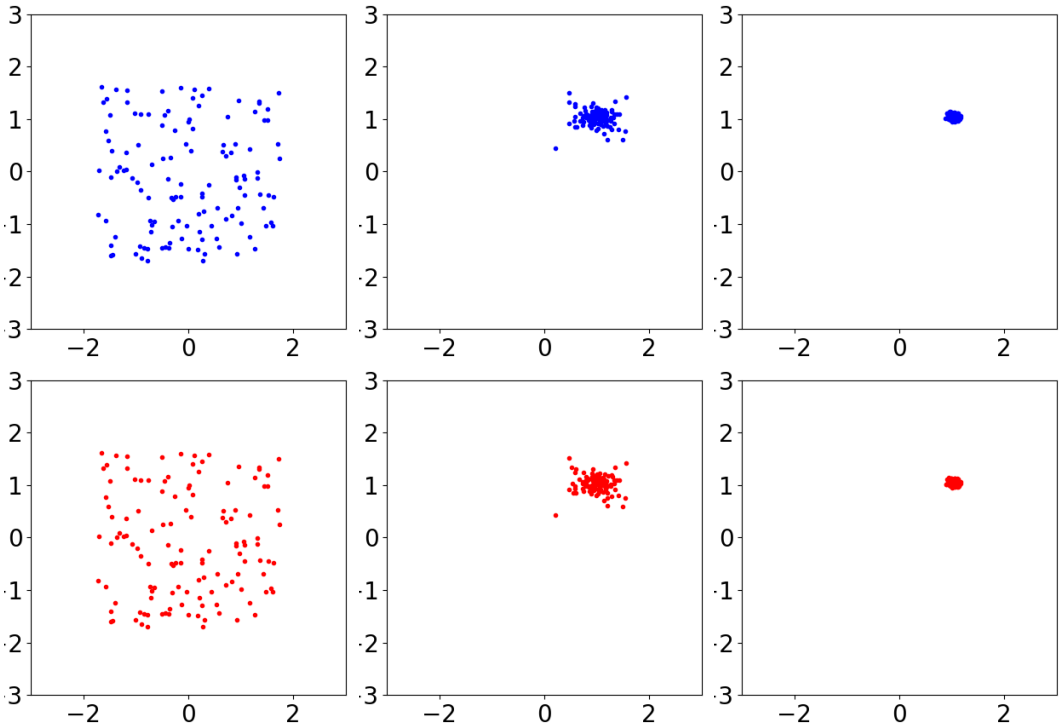

(a) Samples at step $l = 0, 9, 99$

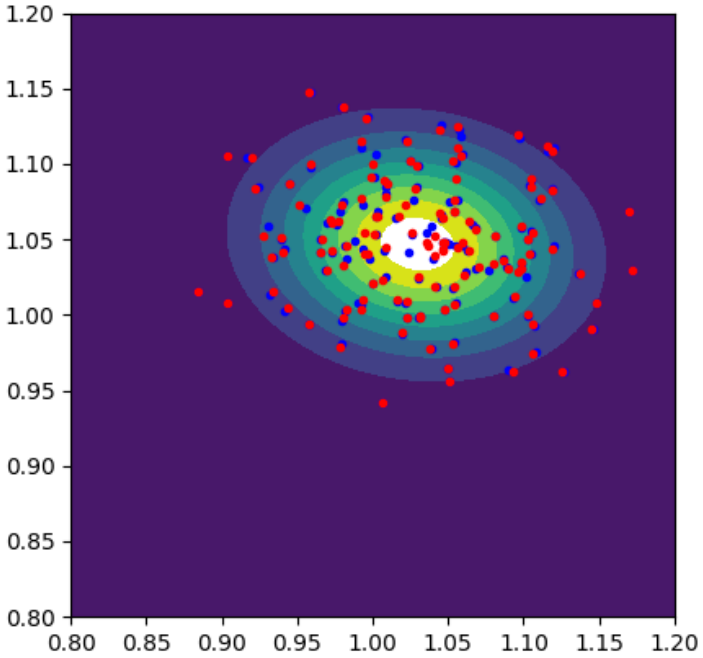

(b) marginal posterior

Figure: Comparison of (128) sample distribution driven by SVGD high-fidelity approximation (blue) and reduced basis approximation (red).

Numerical results: Accuracy

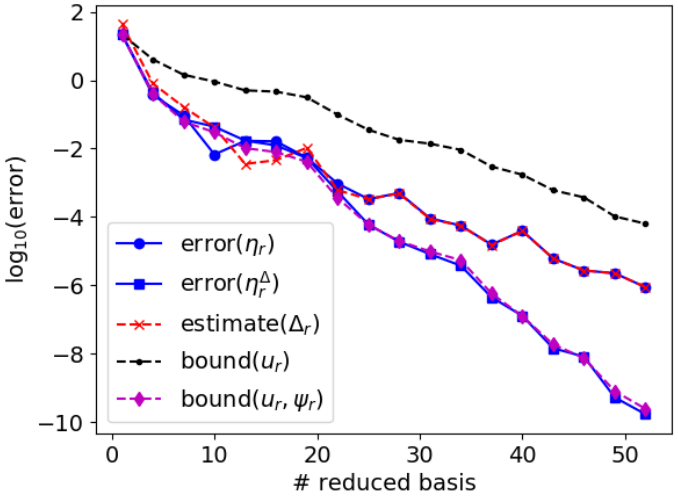

(a) adaptive construction η_y

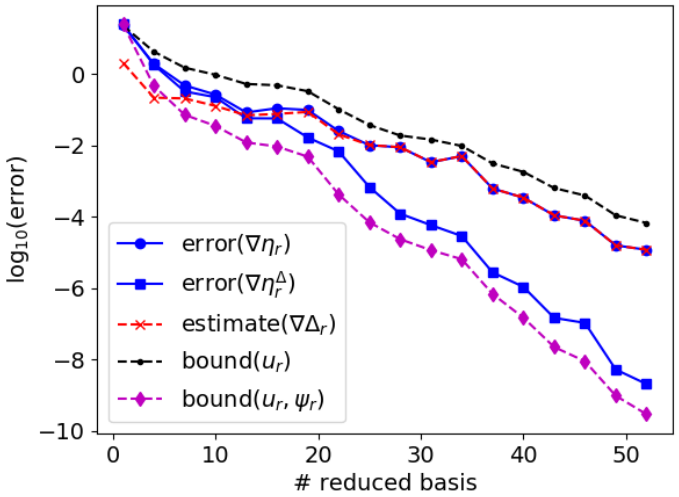

(b) adaptive construction $\nabla_\theta \eta_y$

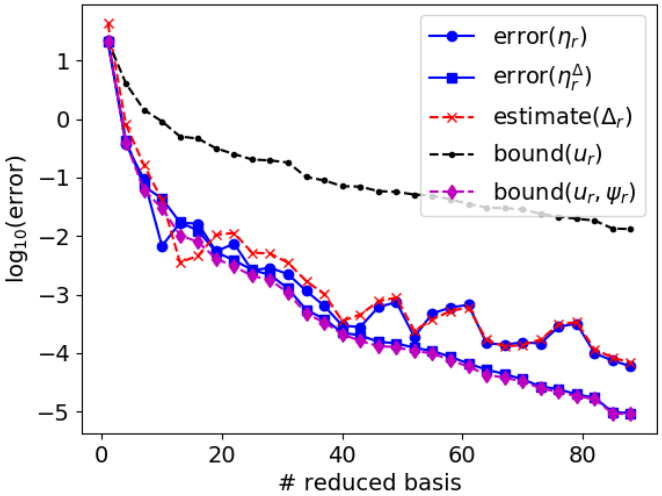

(c) fixed construction η_y

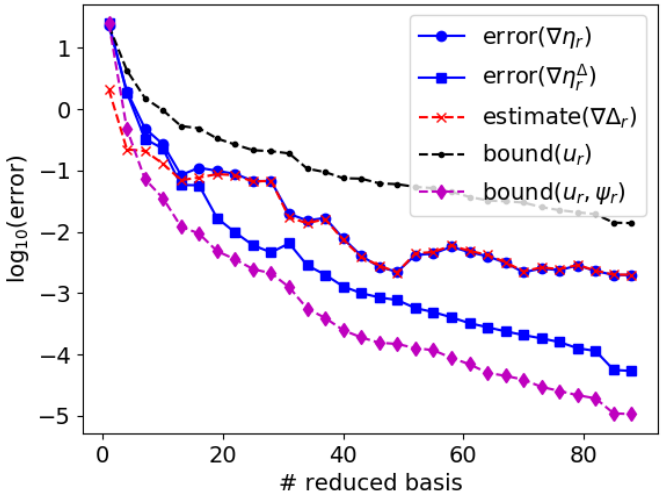

(d) fixed construction $\nabla_\theta \eta_y$

Numerical results: Adaptive greedy algorithm

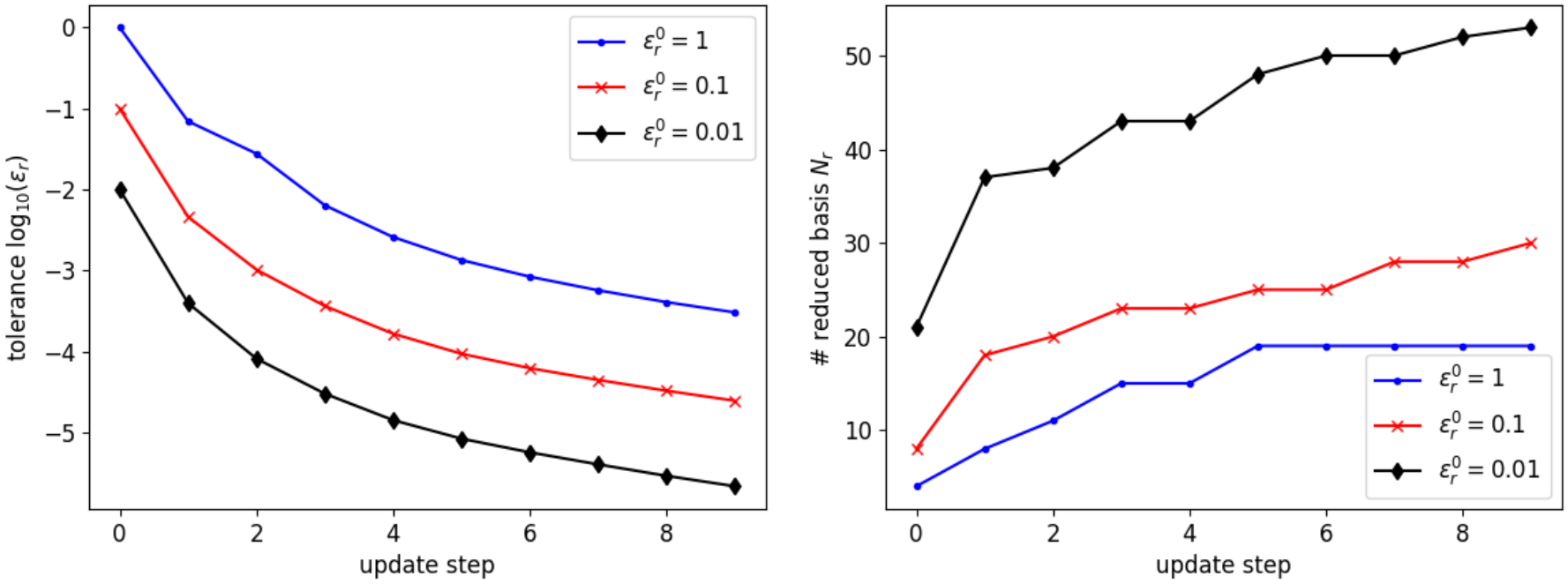

Figure: Tolerances for adaptive greedy algorithm (left);
reduced basis functions for difference initial tolerances (right)

Numerical results: Cost

		FE	adaptive RB			fixed RB
initial tolerance ε_r^0		n/a	1	0.1	0.01	0.00001
$M = 64$	DOF (N_h, N_r)	16641	20	31	49	62
	time to build RB	n/a	4.4	7.1	12.2	15.8
	time for evaluation	1.8×10^3	4.4	4.8	5.8	7.3
	speedup factor	1	203	148	98	62
M=128	DOF (N_h, N_r)	16641	19	30	53	87
	time to build RB	n/a	4.5	7.3	14.3	26.3
	time for evaluation	3.5×10^3	8.3	9.5	11.8	19.2
	speedup factor	1	267	212	137	78

Table: Comparison of high fidelity and reduced basis approximations on degrees of freedom (DOF), CPU time for different tolerances and # samples

P. Chen, O. Ghattas. Stein variational reduced basis Bayesian inversion, 2019.

Summary

Take away message:

- Reduced basis methods reduce the computational cost while preserving physical structure with certified accuracy.
- Leverage goal-oriented adaptive construction of RB.

Ongoing:

- RB for SVN.
- Parameter and state reduction by projected SV + RB.
- Extension to nonlinear and nonaffine problems.

Thank you for your attention!

References I

Beskos, A., Girolami, M., Lan, S., Farrell, P. E., and Stuart, A. M. (2017).
Geometric mcmc for infinite-dimensional inverse problems.
Journal of Computational Physics, 335:327 – 351.

Bui-Thanh, T., Ghattas, O., Martin, J., and Stadler, G. (2013).
A computational framework for infinite-dimensional bayesian inverse problems part I: The linearized case, with application to global seismic inversion.
SIAM Journal on Scientific Computing, 35(6):A2494–A2523.

Bui-Thanh, T. and Girolami, M. (2014).
Solving large-scale pde-constrained bayesian inverse problems with riemann manifold hamiltonian monte carlo.
Inverse Problems, 30(11):114014.

References II

Chen, P. and Ghattas, O. (2019).
Stein variational reduced basis Bayesian inversion.
in preparation.

Chen, P. and Schwab, C. (2016).
Sparse-grid, reduced-basis Bayesian inversion: Nonaffine-parametric nonlinear equations.
Journal of Computational Physics, 316:470 – 503.

Chen, P., Villa, U., and Ghattas, O. (2017).
Hessian-based adaptive sparse quadrature for infinite-dimensional Bayesian inverse problems.
Computer Methods in Applied Mechanics and Engineering, 327:147–172.

References III

Chen, P., Wu, K., Chen, J., O'Leary-Roseberry, T., and Ghattas, O. (2019).
Projected stein variational Newton: A fast and scalable Bayesian inference method in high dimensions.
arXiv preprint arXiv:1901.08659.

Cui, T., Marzouk, Y., and Willcox, K. (2015).
Data-driven model reduction for the bayesian solution of inverse problems.
International Journal for Numerical Methods in Engineering, 102(5):966–990.

References IV

Detommaso, G., Cui, T., Marzouk, Y., Spantini, A., and Scheichl, R. (2018).
A stein variational Newton method.
In *Advances in Neural Information Processing Systems*, pages 9187–9197.

El Moselhy, T. and Marzouk, Y. (2012).
Bayesian inference with optimal maps.
Journal of Computational Physics.

Farcas, I.-G., Latz, J., Ullmann, E., Neckel, T., and Bunagrtz, H.-J. (2019).
Multilevel adaptive sparse Leja approximations for Bayesian inverse problems.
arXiv preprint arXiv:1904.12204.

References V

Gantner, R. N. and Schwab, C. (2016).
Computational higher order quasi-Monte Carlo integration.
In *Monte Carlo and Quasi-Monte Carlo Methods*, pages 271–288. Springer.

Girolami, M. and Calderhead, B. (2011).
Riemann manifold langevin and hamiltonian monte carlo methods.
Journal of the Royal Statistical Society: Series B (Statistical Methodology), 73(2):123–214.

Lan, S., Bui-Thanh, T., Christie, M., and Girolami, M. (2016).
Emulation of higher-order tensors in manifold monte carlo methods for bayesian inverse problems.
Journal of Computational Physics, 308:81–101.

References VI

Lassila, T., Manzoni, A., Quarteroni, A., and Rozza, G. (2013).
A reduced computational and geometrical framework for inverse problems in hemodynamics.
International journal for numerical methods in biomedical engineering, 29(7):741–776.

Lieberman, C., Willcox, K., and Ghattas, O. (2010).
Parameter and state model reduction for large-scale statistical inverse problems.
SIAM Journal on Scientific Computing, 32(5):2523–2542.

Liu, Q. and Wang, D. (2016).
Stein variational gradient descent: A general purpose Bayesian inference algorithm.
In *Advances In Neural Information Processing Systems*, pages 2378–2386.

References VII

Martin, J., Wilcox, L., Burstedde, C., and Ghattas, O. (2012).
A stochastic Newton MCMC method for large-scale statistical inverse problems with application to seismic inversion.
SIAM Journal on Scientific Computing, 34(3):A1460–A1487.

Marzouk, Y., Najm, H., and Rahn, L. (2007).
Stochastic spectral methods for efficient bayesian solution of inverse problems.
Journal of Computational Physics, 224(2):560–586.

Marzouk, Y. and Xiu, D. (2009).
A stochastic collocation approach to Bayesian inference in inverse problems.
Communications in Computational Physics, 6(4):826–847.

References VIII

Nguyen, C., Rozza, G., Huynh, D., and Patera, A. (2010).
Reduced basis approximation and a posteriori error estimation for parametrized parabolic pdes; application to real-time bayesian parameter estimation.
Technical report, John Wiley & Sons.

Oliver, D. S. (2017).
Metropolized randomized maximum likelihood for improved sampling from multimodal distributions.
SIAM/ASA Journal on Uncertainty Quantification, 5(1):259–277.

Rezende, D. J. and Mohamed, S. (2015).
Variational inference with normalizing flows.
arXiv preprint arXiv:1505.05770.

References IX

Schillings, C. and Schwab, C. (2013).
Sparse, adaptive smolyak quadratures for bayesian inverse problems.
Inverse Problems, 29(6).

Schillings, C., Sprungk, B., and Wacker, P. (2019).
On the convergence of the Laplace approximation and noise-level-robustness of Laplace-based Monte Carlo methods for Bayesian inverse problems.
arXiv preprint arXiv:1901.03958.

Schwab, C. and Stuart, A. (2012).
Sparse deterministic approximation of bayesian inverse problems.
Inverse Problems, 28(4):045003.

References X

Spantini, A., Bigoni, D., and Marzouk, Y. (2018).
Inference via low-dimensional couplings.
The Journal of Machine Learning Research, 19(1):2639–2709.

Stuart, A., Voss, J., and Wilberg, P. (2004).
Conditional path sampling of sdes and the langevin mcmc method.
Communications in Mathematical Sciences, 2(4):685–697.

Wang, J. and Zabaras, N. (2005).
Using Bayesian statistics in the estimation of heat source in radiation.
International journal of heat and mass transfer, 48(1):15–29.

Wang, K., Bui-Thanh, T., and Ghattas, O. (2018).
A randomized maximum a posteriori method for posterior sampling of high dimensional nonlinear Bayesian inverse problems.
SIAM Journal on Scientific Computing, 40(1):A142–A171.

References XI

Wang, Z., Cui, T., Bardsley, J., and Marzouk, Y. (2019).
Scalable optimization-based sampling on function space.
arXiv preprint arXiv:1903.00870.

Thank you for your attention!